THE JOURNAL OF PHYSICAL CHEMISTRY B

REVIEW ARTICLE

pubs.acs.org/JPCB

# Multireference and Multiconfiguration Ab Initio Methods in Heme-Related Systems: What Have We Learned So Far?

Hui Chen,* Wenzhen Lai, and Sason Shaik*

Institute of Chemistry and the Lise Meitner-Minerva Center for Computational Quantum Chemistry, Hebrew University of Jerusalem, Givat Ram Campus, 91904 Jerusalem, Israel

**ABSTRACT:** This work reviews the recent applications of ab initio multireference/multiconfiguration (MR/MC) electronic structure methods to heme-related systems, involving tetra-, penta-, and hexa-coordinate species, as well as the high-valent iron-oxo species. The current accuracy of these methods in the various systems is discussed, with special attention to potential sources of systematic errors. Thus, the review summarizes and tries to rationalize the key elements of MR/MC calculations, namely, the choice of the employed active space, especially the so-called double-shell effect that has already been recognized to be important in transition-metal-containing systems, and the impact of these elements on the spin-state energetics of heme species, as well as on the bonding mechanism of small molecules to the heme. It is shown that expansion of the MC wave function into one based on localized orbitals provides a compact and insightful view on some otherwise complex electronic structures. The effects of protein environment on the MR/MC results are summarized for the few available quantum mechanical/molecular mechanical (QM/MM) studies. Comparisons with corresponding DFT results are also made wherever available. Potential future directions are proposed.

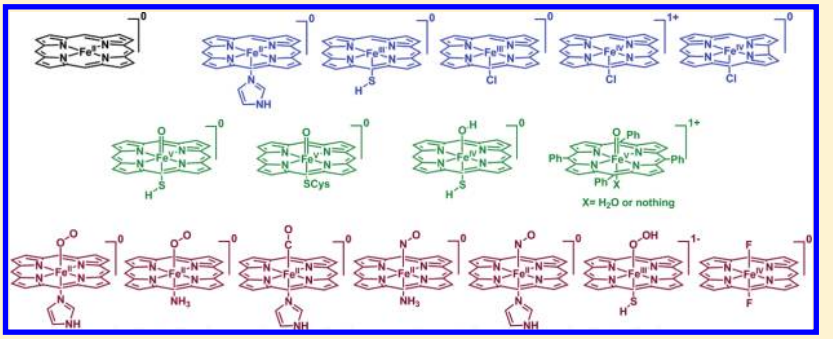


## 1. INTRODUCTION

It is estimated that one-third of all proteins are metalloproteins and a significant fraction of them are heme proteins and enzymes.[1] As such, understanding the structure and reactivity of heme proteins and enzymes has evolved to be an important area of bioinorganic chemistry. Until now, density functional theory (DFT) has played the dominant role in the interplay of theoretical and experimental efforts toward achieving this requisite understanding of the chemistry of heme species.[2−18] Whereas DFT is appropriate for model systems, the enzymatic species require a combined quantum mechanical/molecular mechanical (QM/MM) approach,[19−29] using DFT as the QM method for describing the active species and MM force fields to account as realistically as possible for the effect of protein environment. Indeed, QM(DFT)/MM studies have appeared by now for many heme proteins, e.g., cytochrome P450,[30] cytochrome *c* peroxidase (CcP) and ascorbate peroxidase (APX),[31−35] catalase and catalase-peroxidase,[36−39] horseradish peroxidase (HRP),[40−47] nitric oxide synthase (NOS),[48−51] heme oxygenase (HO),[52,53] myoglobin (Mb) and hemoglobin (Hb),[54−63] truncated Hb,[64−67] chloroperoxidase (CPO),[68−71] and tryptophan/indoleamine 2,3-dioxygenase (TDO/IDO).[72−74]

Even though DFT and DFT/MM have caused a renaissance in heme chemistry, there has always been a looming doubt whether DFT is sufficiently reliable to handle all the open-shell species of heme systems. The almost unanimous view is that validation would eventually be required by high-level electronic structure methods that take into account electron correlation in a systematic manner. As such, the past years have marked a significant turn toward the use of ab initio wave-function-based methods, which handle explicitly the multireference character of the electronic structures. A major drive in this direction has been the development of the efficient algorithms and increase of computer power, which has enabled systems as large as heme complexes to be treated using ab initio multireference/multiconfiguration (MR/MC) quantum chemistry methods, as well as QM(MR/MC)/MM methods. Since the number of such studies keeps growing, it was deemed timely to review this topic, provide a snapshot of a rapidly growing subfield, and answer the title question: What have we learned so far?

As such, the present paper reviews the various MR/MC theoretic investigations of heme enzymes and heme-related macrocyclic systems like iron corrole, and wherever possible it provides the insight gained from these calculations on these complex systems. As one of the important goals of these ab initio calculations is the validation and testing of the widely employed

**Received:** October 19, 2010
**Revised:** December 15, 2010
**Published:** February 24, 2011

**Scheme 1. Heme-Related Systems Reviewed Herein**[a]

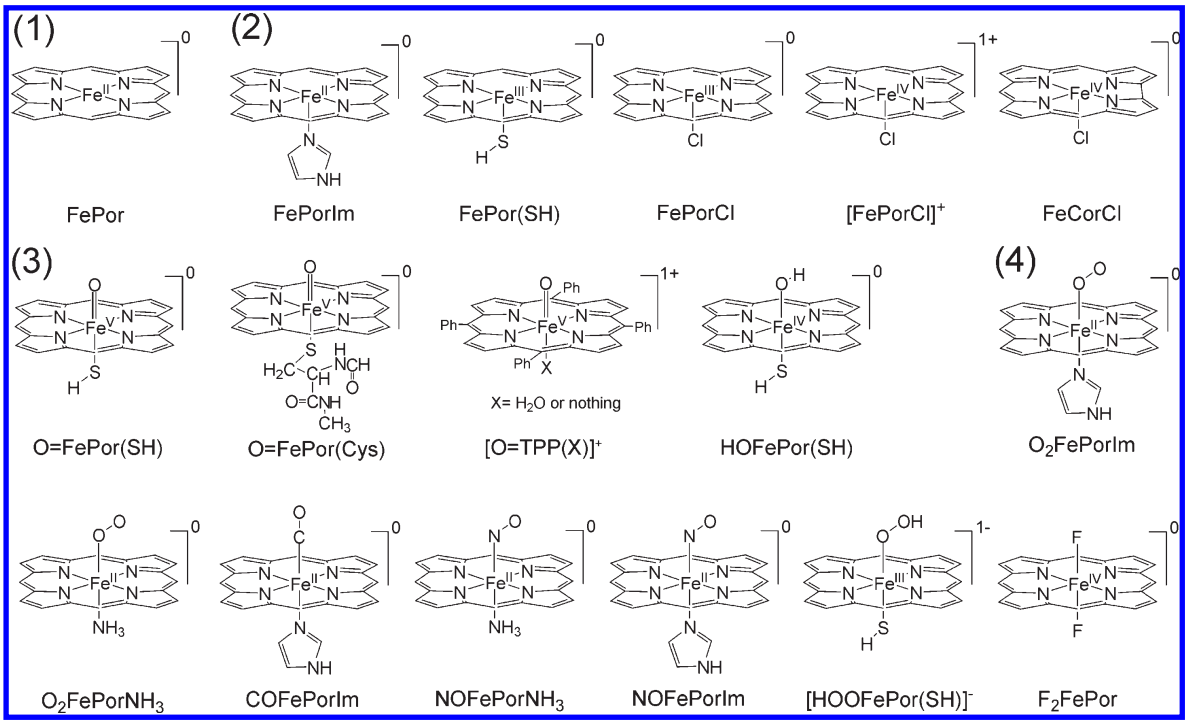


[a] (1) Tetra-coordinate; (2) penta-coordinate; (3) hexa-coordinate with oxygen atom as sixth ligand; (4) hexa-coordinate heme with non-oxygen atom or diatomic/triatomic molecule as distal/sixth ligand.

DFT methods, comparisons of MR/MC calculations to the corresponding DFT calculations are made wherever available. By necessity, this field is at the moment more eclectic than systematic, and therefore our review will attempt to paint some systematics into the many studies by (a) classifying the studies according to chemical species that occur in enzymes and constitute targets for synthetic models designed to mimic these enzymes and (b) focusing on multireference methods and their minimal technical requirements to provide reliable results.

## 2. SYSTEMS AND COVERAGE

**A. Systems.** Scheme 1 above shows the division of the reviewed species into the following categories: (1) tetra-coordinate heme (without axial and sixth ligands); (2) penta-coordinate heme and related complexes; (3) hexa-coordinate heme with an oxygen atom as the sixth ligand, i.e., high-valent iron-oxo hemes; (4) hexa-coordinate heme with nonoxygen atoms or a diatomic molecule as the axial/sixth ligand.

Note that the oxidation numbers on iron, in Scheme 1, are formal oxidation states, not charges. Additionally, using the same oxidation-state formalism, the porphinato (Por) has two formal negative charges whereas the corrolato (Cor) has three formal negative charges. The coverage of these species is limited to systems where the protoporphyrin-IX macrocycle is modeled at least by the porphine ring. Studies including further simplifications of the macrocycle are not discussed.

**B. MR/MC Methods Coverage and Glossary.** The coverage of the review is limited to MR/MC QM and QM/MM ab initio calculations. Earlier semiempirical,[75−79] ab initio GVB/GVB-CI,[80,81] single-reference-based configuration interaction (CI),[82,83] and symmetric adapted cluster and configuration interaction (SAC/SAC-CI) studies[84−87] are not reviewed here but may be mentioned in passing.

The types of MR/MC methods that will be discussed here all involve a MC wave function that accounts for long-range (static) correlation of the electrons in bonds and orbitals, most of which are followed by some MR perturbation- or configuration interaction-theoretic treatments that retrieves dynamic correlation effects. The MC wave function used in most of the calculations for the systems in Scheme 1 is based on the complete active space self-consistent field (CASSCF) method.[88] An active space is a molecular orbital (MO) window defined by two indices, ($N_{elec}$, $N_{orb}$), where "$N_{elec}$" is the number of active electrons and "$N_{orb}$" is the number of active MOs. The term "complete" denotes the fact that all possible arrangements of active electrons in the active orbitals in the active-space window are included. Since the heart of MR/MC calculations is the active space, we shall summarize the gained experience for designing active space in heme systems, with a focus on the "double-shell" effect,[89] whereby the 3d orbitals of iron in the active space are reinforced by a shell of "4d" orbitals. As shall be seen, this "double shell" is necessary to handle the static and dynamic correlation of filled d orbitals, and to obtain thereby reasonable accuracy.

On the basis of MC wave function, the dynamic correlation is introduced usually by means of MR second-order perturbation (MRPT2) or configuration interaction singles and doubles theory (MRCISD), with the former being computationally more effective than the latter. The MRPT2, in contrast to its single-reference analogue MP2, is not uniquely defined. Thus, there exist a variety of implementations, which differ by the zero-order Hamiltonian and by the perturbation procedures. The most popular MR second-order perturbation method, so-called CASPT2, was developed in the Lund group of the late Björn

Roos.[90,91] Another one, which had also been employed in relatively large heme-related systems, is Hirao's MRMP2 method that differs from CASPT2 mainly by the zero-order Hamiltonian and configuration contraction.[92,93] Due to the higher computational cost compared with MRPT2, at present, the MR configuration interaction methods like MRCISD cannot treat systems of the size discussed in this review, unless some further approximation is made in the theory. Such approximation of MRCISD was done in the difference-dedicated configuration interaction (DDCI) approach, which omits some types of configurations whose contributions do not affect the energy difference between electronic states.[94−96]

To bypass the time and storage space consumption of the electron−electron repulsion/exchange integrals, whose number increases explosively with increasing basis set and enlarging system magnitude, one uses various techniques. A popular such technique is the Cholesky decomposition (CD), which was developed and implemented as in MOLCAS[97] to reduce computational time and disk storage needs, thus enabling one to calculate larger systems and to use more extended basis sets than before with many methods including CASSCF and CASPT2.[98] The other popular technique is density fitting (DF)/resolution-of-the-identity (RI), as implemented in Turbomole,[99] ORCA,[100] MOLCAS,[97] etc.

Since the MR/MC calculations usually treat many states of a given species and compare their energetics, a balanced treatment of various states is important. A large number of CASPT2 applications[89,101] revealed that the method systematically overstabilizes states having more unpaired electrons. This preference is rooted in the use of the same averaged Fock operators for α and $\beta$ electrons. To correct for this imbalance, initial attempts were made to modify the zeroth-order Hamiltonian known as g1, g2, and g3 modifications.[102] These modifications, while they may improve the performance of CASPT2 in cases where the original CASPT2 zero-order Hamiltonian encounters problems, have nevertheless limitations that may require in some cases the use of very large level shifts to avoid the intruder state problem.

Roos and his co-workers[103] introduced another approach, which avoids the limitation of the zero-order Hamiltonians of g1, g2, and g3 and addresses the systematic error of the original CASPT2 formalism for states having different numbers of unpaired electrons. This method of modifying the zero-order Hamiltonians is called IPEA shift, and it is associated with the shifting of partially occupied orbital energies when exciting electrons into or out of the respective active orbitals. The standard IPEA-shift constant (0.25 au) was determined by the optimal performance CASPT2 in eliminating the systematic error of the original zero-order Hamiltonian, for bond dissociation energies of small molecules, and spectroscopic constants, excitation energies, and ionization energies of transition metal atoms. This IPEA shift of 0.25 au is the current default option in the MOLCAS suite of programs.[104] However, the user should be alerted to the possibility that this "remedy" is not a panacea, and hence may lead to less successful results for specific systems as found recently in some ferrous pseudooctahedral $FeN_6$ spin crossover systems.[105]

## 3. REVIEWING THE MR/MC CALCULATIONS OF THE SPECIES TYPES IN SCHEME 1

**i. Tetra-Coordinate Heme Species.** Even though tetra-coordinate heme complexes do not figure much in heme enzymes, still the related porphyrin systems constitute important building blocks in supramolecular chemistry and nanochemistry.[106−110] Therefore, we start with these relatively simpler systems where no axial ligands are presented in the coordination sphere of the ferrous, Fe(II), ion. Hirao et al.[111] performed an early investigation of a Fe(II)Por model system in $D_{4h}$ symmetry using the MRMP2 method[92,93] based on a CASSCF reference wave function. Geometries for various states were optimized by CASSCF(6,5) calculation, wherein six electrons in the five iron 3d orbitals were included in the active space. The basis set used was of double-ζ quality for both Fe and main group elements without polarization basis functions. The active space for the MRMP2/CASSCF calculations involved the five 3d orbitals and six $\pi$-type orbitals of the porphine, labeled as MRMP2(10,11).

**Scheme 2. The Five 3d Orbitals[a] in Fe(II)Por and Their Occupancy in the Leading Configuration of the $^5A_{1g}$ State**

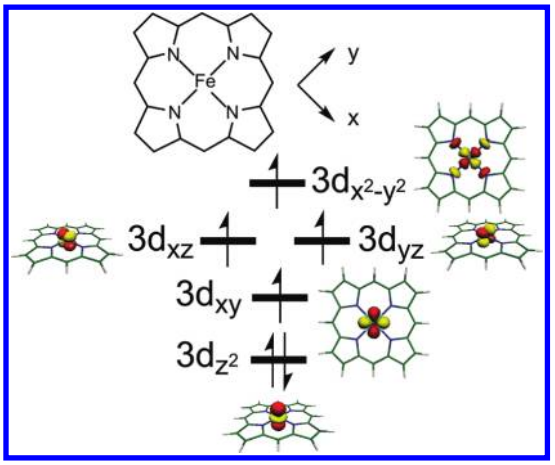


[a] The Cartesian coordinate system defines the orbital labels, which are used throughout the review unless specified otherwise.

The MRMP2 calculations showed that the lowest state of the Fe(II)Por species is the quintet state ($^5A_{1g}$) with a leading configuration $(d_{z^2})^2(d_{x^2-y^2})^1(d_{xy})^1(d_{yz})^1(d_{xz})^1$ which is depicted in Scheme 2, and which lies below the next two quintet states $^5E_g$ and $^5B_{2g}$ by 4.3 kcal/mol at least. Additionally, two lowest triplet states, $^3E_g$ with $(d_{z^2})^1(d_{x^2-y^2})^0(d_{xy})^2(d_{yz})^1(d_{xz})^2$ as a main configuration and $^3A_{2g}$ with $(d_{z^2})^2(d_{x^2-y^2})^0(d_{xy})^2(d_{yz})^1(d_{xz})^1$, were found to be higher than all three quintet states mentioned above, and lie about 8.5 and 13.8 kcal/mol above the ground state $^5A_{1g}$.[111] Since this result conflicts with experimental suggestions that the ground state for substituted ferrous−porphine complexes is the triplet state (either $^3A_{2g}$ or $^3E_g$),[112−115] it was apparent that the computational level is inadequate. Hence, subsequently, Hirao and Lindh et al. performed CASPT2 calculations[116] on the Fe(II)−porphine system and augmented the previously used basis set[111] by inclusion of polarization functions on all non-hydrogen atoms (Wachter's basis set augmented with f polarization for iron contracted as [8s6p4d1f] and cc-pVDZ for other non-hydrogen atoms contracted as [3s2p1d]). The active space was also enlarged to (14,13), by including two more $\pi$-type porphine orbitals compared with the previous calculations.[111] Still, however, this CASPT2 calculation further augmented the stability of the $^5A_{1g}$ state, and placed it 19.2 kcal/mol lower than the lowest triplet ($^3A_{2g}$) state. Relativistic calculations were found to have a very small effect on the quintet-states energy, relative to other

spin states (less than 2.0 kcal/mol variation relative to $^3A_{2g}$), and almost no effect on the triplet and singlet states. As found before in earlier theoretical studies,[75,82,117] geometric parameters, and mainly the Fe−$N_{Por}$ bond length, were important in setting the quintet−triplet splitting. After comparison with related experimental structures, Hirao et al. concluded that the CASSCF(6,6) geometry optimization could be the reason that the CASPT2 calculations favored $^5A_{1g}$ over $^3A_{2g}$.

To further understand the source of the apparent inconsistency of the above CASPT2 results with experiment, Pierloot performed a comparative study of Fe(II)−porphine, employing CASPT2 with three kinds of active spaces.[118] In addition to the (14,13) and (6,5) used by Hirao et al.,[116] Pierloot tried also a new active space (8,11), wherein one set of five 4d orbitals and one Fe−$N_{Por}$ $\sigma$ bonding orbital were added into the (6,5) active space of the iron 3d orbitals to account for the double-shell effect. The "double shell" serves to reduce the electron−electron repulsion in the doubly occupied 3d orbitals, and thereby should stabilize triplet states, which include double occupancy (consult Scheme 2). The inclusion of the Fe−$N_{Por}$ $\sigma$ bonding orbital, in addition to the Fe−$N_{Por}$ $\sigma^*$ antibonding orbital ($3d_{x^2-y^2}$) served to account properly for nondynamic correlation in the Fe−$N_{Por}$ bonds due to their possible covalent bonding character. As such, the geometries were optimized at the CASPT2(8,11) level for all four considered states, quintet ($^5E_g$ and $^5A_{1g}$) and triplet ($^3A_{2g}$ or $^3E_g$), and the basis set for iron and its first coordinate sphere (four N atoms) was further augmented to be at least of polarized triple-$\zeta$ quality ([7s6p5d2f1g] for iron and [4s3p1d] for N atoms).[118] Interestingly, the calculated CASPT2/CASSCF(8,11) adiabatic gap between lowest quintet and triplet state, $^5A_{1g}$−$^3A_{2g}$,[118] *shrunk by about 9 kcal/mol*, compared with the previous calculations, which did not include the "double shell".[116] Thus, in the studied Fe(II) system, the double-shell effect is more important than the increase of the active space with more porphine orbitals. While this double-shell effect did not manage to resolve the inconsistency with experiment, since the gap was still 10.1 kcal/mol in the wrong direction, it clearly showed that an important way to improve the results vis-à-vis experiment must involve the double-shell effect in future calculations of heme systems.

Recently, Radoń and Pierloot reported their new CASPT2 calculations on the Fe(II)−porphine system[119] using a larger basis set, of multiple polarized triple-$\zeta$ quality for iron and its first coordinate sphere, and polarized triple-$\zeta$ quality for C and H atoms (Fe, [7s6p5d3f2g1h]; O, [4s3p2d1f]; N, [4s3p2d1f]; C, [4s3p1d]; H, [3s1p]). The iron 3s3p semicore electrons were correlated in the CASPT2 calculations, and the scalar relativistic effect was also considered via the second-order Douglas−Kroll−Hess (DKH) transformation.[120] The same (8,11) active space as before[118] was used. The standard IPEA-shifted (0.25 au) zero-order Hamiltonian[103] was employed during the CASPT2 calculation. Using optimized DFT geometries, with PBE0 and BP86 density functionals, the calculated adiabatic quintet−triplet ($^5A_{1g}$−$^3A_{2g}$)[121] gap of Fe(II)Por further shrunk to 5.1 kcal/mol (no zero-point energy correction was included, to be consistent with previous results). To quantify the increment of the basis set quality vs other calculation settings, the authors[119] also did the calculations with a smaller basis set of similar quality with previous calculation[118] while keeping all the other settings unchanged. The so calculated quintet−triplet gap was 7.5 kcal/mol vs 5.1 kcal/mol with the larger basis set. As such, judging from the results published by the authors, the basis set improvement accounts for a 2.4 kcal/mol reduction in the quintet−triplet gap (from 7.5 to 5.1 kcal/mol), while the rest of the 2.6 kcal/mol gap lowering (from previous 10.1 to the current 7.5 kcal/mol) must derive from three other different calculation settings, i.e., scalar relativistic effect, iron 3s3p correlation, and IPEA-shifted zero-order Hamiltonian. However, as was shown later using CASPT2 calculation on the related Fe(II)PorIm (Im is imidazole that models a histidine ligand) system,[122] the iron 3s3p correction should have almost no effect on the quintet−triplet gap. In addition, the scalar relativistic effect could even increase the quintet−triplet gap ($^5A_{1g}$−$^3A_{2g}$) by about 1.8 kcal/mol according to Hirao et al.'s calculations.[116] Thus, among the three different calculation settings, the IPEA-shifted zero-order Hamiltonian reduces the gap by 2.6 kcal/mol in the correct direction. However, the IPEA shift still does not lead to agreement with experiment.

Thus, from the above discussions of the relatively simple Fe(II)−porphine system, it is clear that, despite the great efforts and associated improvements, still CASPT2 cannot reproduce the triplet state as ground state. The most updated result for the adiabatic quintet−triplet gap (without ZPE correction) calculated with a large basis set and the IPEA-shifted zero-order Hamiltonian formalism of CASPT2 is 5.1 kcal/mol. This result led Radoń and Pierloot to conclude that a systematic error, of at least 5 kcal/mol in favor of the high-spin state, still exists in CASPT2 calculations for the quintet−triplet gap problem in the Fe(II)−porphine system.[119,122] On the contrary, many density functionals like BP86, B3LYP, OLYP, OPBE,[119,123−125] and some others[126] reproduce the correct triplet state as a ground state. As shown above, the quintet−triplet gap for Fe(II)−porphine involves states with different orbital occupancies, $(d_{x^2-y^2})^1(d_{xy})^1$ and $(d_{x^2-y^2})^0(d_{xy})^2$. Obviously, this is a case of states with a different number of unpaired electrons, and is subject to the imbalanced treatment issue of the CASPT2 method. Thus, the difficulty in accurate calculations of this gap by CASPT2 could be associated with the accuracy of the IPEA-shifted zero-order Hamiltonian of CASPT2 in the current system. We will see similar cases in the sections below and will revisit this point later in this review.

**ii. Penta-Coordinate Heme and Related Complexes.** Penta-coordinate systems ((2) in Scheme 1) are important in the catalytic cycles of most heme enzymes, since their vacant coordination site is used to ligate oxygen-rich molecules (like $O_2$, $H_2O_2$, etc.) or substrates en route to oxidation. Let us then turn to discuss some of these penta-coordinate heme systems. In systems like Fe(III)PorCl, one deals with three spin states with $S = {}^1/_2$, ${}^3/_2$, and ${}^5/_2$. However, in the 1e-oxidized species, e.g., $[FePorCl]^+$, there are additionally two different electromers, which reflect the relative donor ability of the Fe(III) vs the porphine ligand: one being Fe(III)/$Por^{\bullet+}$ and the other a ferryl high-valent Fe(IV)/Por type. Moreover, the singly occupied orbital in $Por^{\bullet+}$ can be in the $a_{2u}$ or $a_{1u}$ orbitals, which are depicted in Figure 1.

In 2003, Ghosh and Taylor et al. compared the Fe(III)PorCl and $[FePorCl]^+$ systems using the CASPT2 and DFT methods.[127,128] The authors used a (9,9) active space (four porphine $\pi$ orbitals and five Fe 3d orbitals) and employed a polarized double-$\zeta$ quality basis set on all atoms except iron and additional diffuse functions on Cl (Fe, [6s5p4d3f2g]; O/N/C, [3s2p1d]; Cl, [5s4p2d]; H, [2s1p]). The geometries were optimized with B3LYP and a polarized triple-$\zeta$ quality basis set with an extra diffuse set on Cl. The CASPT2 calculations utilized the g3 zeroth-order Hamiltonian[102] and included 3s3p

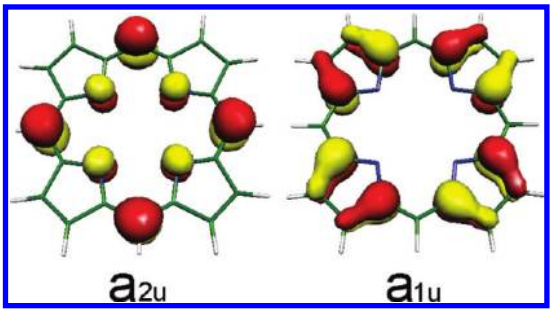


**Figure 1.** The low-lying $\pi$-type molecular orbitals (MO) $a_{2u}$ and $a_{1u}$ of the porphine ring, either of which can be oxidized to form an open-shell $Por^{\bullet+}$.

correlation for iron. In the case of Fe(III)PorCl, the CASPT2 results predicted that the $S = {}^5/_2$ state (with five unpaired electrons in the d-type orbitals) is adiabatically 19.6 kcal/mol lower than $S = {}^3/_2$ (with three unpaired d-electrons), whereas B3LYP predicts these two states to be of comparable energy ($S = {}^3/_2$ is 1.8 kcal/mol higher than $S = {}^5/_2$).

For the $[FePorCl]^+$ species, the CASPT2 results suggested that the ground state is the quintet-state $[Fe(III)Por^{\bullet+}Cl]^+$ electromer, having antiferromagnetic coupling between an $S = {}^5/_2$ Fe(III) and an $S = {}^1/_2$ porphine cation radical with a singly occupied $a_{2u}$ orbital. The $[Fe(IV)PorCl]^+$ electromer was found to lie more than 35 kcal/mol above the ground Fe(III) state $[Fe(III)Por^{\bullet+}Cl]^+$, in qualitative agreement with B3LYP results. The main difference between CASPT2 and B3LYP was the smaller B3LYP gap, vis-à-vis CASPT2, between the $[Fe(III)Por^{\bullet+}Cl]^+$ states with singly occupied $a_{2u}$ ($A_{2u}$) and those characterized by singly occupied $a_{1u}$ ($A_{1u}$).

In 2005, Ghosh and Taylor published their study of the $FePorF_2$ system.[129] Although $FePorF_2$ is hexa-coordinate, its similarity to a penta-coordinate system like $[FePorCl]^+$, in terms of the two electromeric possibilities, requires some discussion herein. All the CASPT2 calculation settings were the same as those for $[FePorCl]^+$, except for the active space which was (11,11), and included in addition to the (9,9) used for $[FePorCl]^+$,[127] also the $\sigma/\sigma^*$ Fe−F orbitals to account for the nondynamic electronic correlation of the Fe−F bonds. To confirm the results, the authors employed also a larger active space (15,15), which extended the former by four additional porphine $\pi/\pi^*$-type orbitals. In contrast to B3LYP calculations, which predicted an $S = 1$ Fe(IV) ground state, the CASPT2 calculations generated an $[Fe(III)Por^{\bullet+}F_2]$ electromer as the ground state, having an $S = {}^5/_2$ Fe(III) center ferromagnetically coupled to an $S = {}^1/_2$ $a_{2u}$ porphyrin cation radical, and hence a total of $S = 3$ spin quantum number. The gap between the two states was significant (7.1−9.7 kcal/mol) and consistent with the experimental inferences.[130] An antiferromagnetic $S = 2$ Fe(III)$Por^{\bullet+}$ state was found to lie slightly higher (0.9 kcal/mol) than the ferromagnetic ground state.

Recently, Roos, Ghosh, and their co-workers[131] investigated the chloroiron corrole system FeCorCl, using CASPT2. The authors employed a large basis set, with multiple polarized triple-$\zeta$ quality, for iron and its first coordination sphere and a polarized double-$\zeta$ quality basis set for the rest. Scalar relativistic effects were considered by DKH transformation, and the double-shell effect was accounted for using two 4d orbitals in the (14,14) active space. The geometry of the ground state was optimized at the B3LYP/TZP level with $C_s$ symmetry. The CASPT2 results showed that the lowest two states are of Fe(III)$Cor^{\bullet+}$ type, having $S = {}^3/_2$ and $S = {}^5/_2$ Fe(III) centers antiferromagnetically coupled to a corrole cation radical. In agreement with DFT results, the lowest 10 states revealed only Fe(III)$Cor^{\bullet+}$ electromers, whereas no high-valent Fe(IV)Cor states were located within about 1.5 eV from the ground state. Thus, this state pattern of FeCorCl is rather similar to the CASPT2 results of Ghosh for the analogous $[FePorCl]^+$ system discussed above.[127]

The above work of Roos et al.[131] and the work of Radoń et al.,[119] both published in 2008, were the first CASPT2 studies of heme-related systems that employed the Cholesky decomposition (CD) technique,[98] which enables CASPT2/CASSCF application to larger systems of lower molecular symmetry and larger basis sets than before. These studies stimulated later CD-CASPT2 calculations[132] for computationally more demanding heme systems without any symmetry.

In a very recent paper, Pierloot et al.[122] studied the two penta-coordinate heme model systems Fe(III)Por(SH) and Fe(II)-PorIm relevant to heme enzymes using CD-CASPT2. The Fe(III)Por(SH) is a model of a penta-coordinate ferric complex in heme enzymes with a cysteine axial ligand like P450 and CPO, while Fe(II)PorIm is a model of ferrous deoxyheme species in heme enzymes axially ligated with histidine like in Mb and Hb. To test their CASPT2 results against the high level CCSD(T) study of Harvey et al.,[133] the authors used three molecules with truncated porphines, for which CASPT2−CCSD(T) comparisons could be made.

Additionally, Pierloot et al.[122] explored several large basis sets, up to multiple polarized quadruple-$\zeta$ quality basis set for iron and its first coordinate sphere, with a polarized triple-$\zeta$ quality basis set for the rest of the atoms. The B3PW91-optimized geometries (with $C_s$ symmetry) based on Harvey's work[133] were slightly different from previous BP86 and PBE0 optimized ones,[119] but these differences were shown to have hardly any effect on the CASPT2 results. The other computational settings (scalar relativistic effect and iron 3s3p correlation) were similar to the ones in the previous work of the same authors for the Fe(II)Por and Fe(II)PorIm systems.[119] Double-shell effects were included, using five 4d orbitals on iron, thus leading to (10,12)/(11,13) active spaces for Fe(II)PorIm/Fe(III)Por(SH). These active spaces differ by one additional $\pi$ lone pair of the axial sulfur atom in the Fe(III)Por(SH) complex. The interesting results of this work were the following:

(1) For ferric complexes like Fe(III)Por(SH), CASPT2 was very accurate for spin-state energetics compared with CCSD(T), while, for the ferrous complexes like Fe(II)PorIm, it was found that a systematic error (around 5−10 kcal/mol) in favor of the high-spin state is still persistent.

(2) The CASPT2 error could not be eliminated by simply increasing the IPEA shift as done before in some ferrous $FeN_6$ spin crossover systems.[105] Thus, increasing the IPEA shift, which will possibly turn CASPT2 into a semiempirical approach, was not recommended by Pierloot et al.

(3) The calculated relative energies of the triplet state (9.5 kcal/mol) and singlet state (13.7 kcal/mol), for Fe(II)PorIm, were consistent with previous CASPT2 results[119] on slightly different geometries (8.5−8.6 and 13.0−14.0 kcal/mol).

(4) None of the tested density functionals (B3LYP, B3LYP*, OLYP, BP86, TPSS, TPSSh, M06, and M06-L) could provide a consistent accuracy for all model complexes.

As shown in Scheme 3, it is interesting to note that one of the two smaller model systems for Fe(III)Por(SH)[122] (**1-SH**) is of the same type as the one used by Ghosh et al. to perform CCSD(T) calculations for validating the CASPT2 result for Fe(III)PorCl[127,134] (**1-Cl**). For **1-SH**, Harvey et al.[133] calculated a CCSD(T) sextet−quartet gap of 18.8 kcal/mol, quite close to the corresponding CCSD(T) 17.1 kcal/mol gap of **1-Cl** using a slightly smaller basis set calculated by Ghosh et al.,[134] thus confirming the similarity between these two small models. Moreover, the CASPT2 sextet−quartet gap for **1-SH** (19.2 kcal/mol)[122] is also very close to the corresponding CCSD(T) gap (18.8 kcal/mol).[133] However, Pierloot et al.[122] further found that for the real Fe(III)Por(SH) system the CASPT2-computed gap was in fact 6−8 kcal/mol lower than that for **1-SH**. This finding means that small models, like **1-SH** or **1-Cl**, are too oversimplified to represent the corresponding heme systems. Thus, the previous validation of the CASPT2 result for Fe(III)PorCl by its smaller model system **1-Cl**[127] now appears somewhat less compelling. As such, although the conclusion of the sextet being lower than the quartet state of Fe(III)PorCl by significant margin[127] is still not likely to change, the sextet−quartet gap for Fe(III)PorCl is probably overestimated due to lack of the double-shell effect in the active space by including iron 4d orbitals.

**Scheme 3. Small Systems Used to Model the Corresponding Fe(III)Por Complexes: (a) the 1-Cl Model for Fe(III)-PorCl;[127,134] (b) the 1-SH Model for Fe(III)Por(SH)[122]**

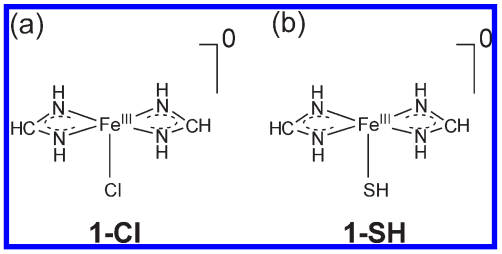


**iii. Hexa-Coordinate High-Valent Iron-Oxo Heme Systems.** High-valent iron-oxo systems like compound I (Cpd I, i.e., the oxoiron(IV)−porphyrin cation radical, shown in Scheme 4) are the active species of most if not all heme enzymes, wherein they perform various oxidative processes. This section is dedicated then to these species. As shown below, due to a very strong and short Fe−O bond ($r_{FeO} \approx 1.6$ Å), Cpd I is different than other heme species, and it poses new difficulties and challenges for MR/MC calculations.

In 2005, Schöneboom et al.[135] published the first MR study of the synthetic Cpd I model system and the P450cam Cpd I, using the difference-dedicated configuration interaction (DDCI2)[96] method in both QM and QM/MM calculations. The models used were O=FePor(Cys) for Cpd I of P450cam (Cys is the axial cysteine residue after its backbone cutting to keep two peptide bonds, see Scheme 1) and $[O{=}FeTPP(X)]^+$ (TPP = *meso*-tetraphenylporphyrin, X = $H_2O$ or no ligand) for the synthetic model. The basis set used was extensive on the central $Fe^{IV}{=}O$ unit, and its first coordinate sphere, which, at the time when this calculation was performed, was a natural choice for such large molecules without any symmetry. B3LYP and B3LYP/MM optimized geometries were used for the synthetic model system and enzymatic species, respectively. For the triradicaloid quartet and doublet ground states of Cpd I, a minimal active space (3,3) was used, which contains the two Fe(IV)=O $\pi^*$ orbitals and one Por $a_{2u}$ orbital.

The main conclusions from the DDCI2 calculations[135] were the following:

(1) The DDCI2/CAS(3,3) computed doublet−quartet splitting of $[O{=}Fe(IV)(TPP^{\bullet+})X]^+$ (X = $H_2O$ or no ligand), which is known experimentally to have a quartet ground state, was found to be smaller than the B3LYP value but in the same direction, quartet-below-doublet.

(2) For Cpd I of P450cam, which by analogy to the same species of the enzyme chloroperoxidase should have a doublet ground state, $^2A_{2u}$, both DDCI2/CAS(3,3)/MM and the B3LYP/MM reproduced the ground-state identity

**Scheme 4. Calculated Orbital Occupancy Diagram of P450 Cpd I in Its Lowest Triradicaloid Doublet and Quartet States Labeled as O=Fe(IV)Por$^{\bullet+}$(Cys)[a]**

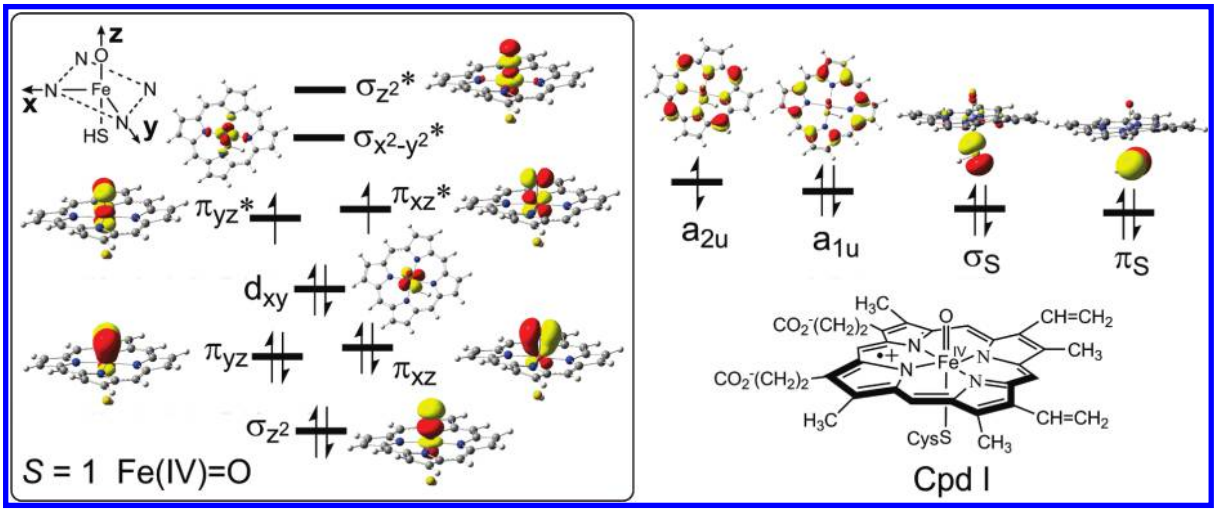


[a] The double-headed arrow in the $a_{2u}$ orbital is for quartet (up) and doublet (down) states, respectively.

**Scheme 5. The Spin Population Feature of DFT(B3LYP) and DDCI2/CASSCF(3,3) QM/MM Calculation for Doublet Cpd I of P450cam[135]**

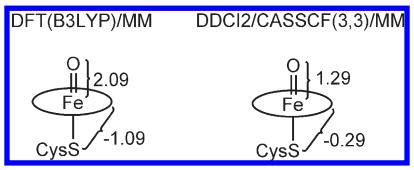


**Scheme 6. A Spin-Adapted DFT Description of Doublet Cpd I**

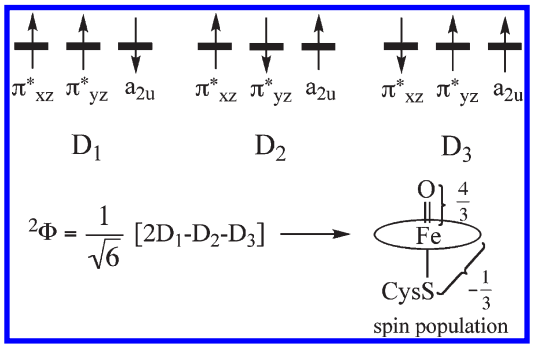


and gave very similar values for the doublet−quartet splitting.

(3) As shown in Scheme 5, DDCI2/CAS(3,3)/MM gave substantially different spin population features of the doublet state compared with DFT/MM. This difference is due to the symmetry broken solution used in DFT for the antiferromagnetically coupled doublet state of Cpd I. Thus, the DFT-derived spin population for the symmetry broken doublet state of Cpd I is not reliable.

Since the spin distribution of the doublet state that emerges from DDCI2/CAS(3,3)/MM does not disclose the triradicaloid nature, which is an important chemical feature of the species, it is appropriate to expand this last point and argue that it is still a triradicaloid despite the different description compared with DFT, and that in fact DFT is still reliable. This is done in Scheme 6. Thus, one of the problems of DFT is the use of a single Kohn−Sham determinant ($D_1$ in Scheme 1) to describe the doublet state. This leads to a broken symmetry solution, since the single determinant is not a definitive spin state and does not properly describe the open-shell singlet coupling of the $a_{2u}$ and $\pi^*$ electrons; therefore, the spin distribution of the $^2A_{2u}$ state is incorrectly evaluated by DFT. However, this can be easily remedied by constructing from the DFT determinant a spin-adapted wave function that describes properly the doublet spin, as shown in Scheme 6. Thus, since the electron in the $a_{2u}$ orbital is singlet-coupled to each one of the electrons in the $\pi^*$ orbitals, the corresponding wave function $^2\Phi$ will involve a combination of spin arrangements, as shown in Scheme 6, which is nothing else but $D_1$ after spin-projection that removes the contaminating quartet component. Therefore, if we order the orbitals as $\pi^*_{xz}\pi^*_{yz}a_{2u}$, the spin arrangements will be $D_1 = |\uparrow\uparrow\downarrow\rangle$, $D_2 = |\uparrow\downarrow\uparrow\rangle$, and $D_3 = |\downarrow\uparrow\uparrow\rangle$, the former having a double coefficient and hence a quadrupled weight compared with the latter two. Since the spin of the $a_{2u}$ electron has spin down with a relative weight of 4 and spin up with a relative weight of 2, the sum is a spin down weight of 2. When we normalize the wave function, the spin distribution in the doublet states should be $^2/_3$ in each of the $\pi^*_{xz}$ and $\pi^*_{yz}$ orbitals and $-^1/_3$ in $a_{2u}$. This distribution in Scheme 6 is close to the DDCI2/CAS(3,3)/MM results and to all subsequent MR/MC calculations. As such, the $^2A_{2u}$ state is described at the correlated level as a triradicaloid with singly occupied $\pi^*_{xz}$, $\pi^*_{yz}$, and $a_{2u}$ orbitals. We may also conclude that spin adaptation of the DFT wave function is sufficient to retrieve these high level results, and since the $^2A_{2u}-^4A_{2u}$ energy gap of the B3LYP/MM is reliable, the DFT method does in fact quite well.

Recently, Neese, Thiel, and their co-workers published a more extensive DDCI2+Q QM/MM study for Cpd I of P450cam using a larger basis set and active space.[136] The QM part for Cpd I is R/O=Fe(IV)Por$^{\bullet+}$(SH), where R is a truncated camphor used in QM/MM calculations. Unfortunately, the large active space (13,12), which includes all O atom bonding orbitals and iron 3d orbitals except $3d_{xy}$ (iron nonbonding orbital), was found to converge only for quartet states but not for doublet states. The results confirmed most of the features found in the former study.[135] However, most puzzling was the result that the $^4A_{1u}$ state was only 1.9 kcal/mol higher than the $^4A_{2u}$ state at the DDCI2+Q level, whereas TD-B3LYP predicts that this gap is more than 10 kcal/mol.

In the same work, the authors also studied the ferric hydroperoxide species called Cpd 0 ([HOOFe(III)Por(SH)]$^-$), which is the precursor of Cpd I in the P450 catalytic cycle, and the ferryl hydroxo species, so-called Cpd II (R•/HOFe(IV)Por(SH)), which is obtained during H-abstraction from the substrate by Cpd I. The DDCI2/MM results for the two species were quite consistent with B3LYP/MM in terms of both relative energetics and electronic structures of low-lying states.

Radoń and Broclawik[137] used CASPT2 to study the Cpd I model system O=Fe(IV)Por$^{\bullet+}$(SH) for P450 in the gas phase. The basis set used was generally of polarized double-ζ quality, which is comparable for iron and its immediate coordination sphere with the one used in the above DDCI2+Q study.[136] Compared with the previous Cpd I studies,[135,136] the authors used a (15,12) active space which included more Por $\pi$-type orbitals and sulfur-based orbitals but lacked the Fe−$N_{Por}$ $\sigma/\sigma^*$ orbitals (the latter being mainly an iron 3d orbital type). The gas-phase calculation of Radoń et al. showed the following trends:

(1) Only multistate CASPT2 calculation, which permits the CASSCF references of the involved multistates to remix perturbatively, could lead to the same ground state identity as DFT calculation.

(2) State-averaged orbitals are not uniformly optimal for all the states. State-specific calculations are more appropriate.

(3) Similar to what was found before in [FePorCl]$^+$,[127] at the CASSCF level, the $A_{1u}$ state (singly occupied $a_{1u}$) is lower than the $A_{2u}$ state in Cpd I. Dynamical correlation inverts this state ordering.

Thus, while each of the above studies of Cpd I contained useful information, as a whole they did not provide a complete rationalizable picture for the electronic structure of Cpd I at the MR/MC level. This is mainly due to the fact that Cpd I has a dense manifold of low-lying states compared with other heme species. The most direct consequence of this complexity is that the coverage of the MR/MC study is highly dependent on the active space used. The work of Radoń et al.[137] also suggested that,

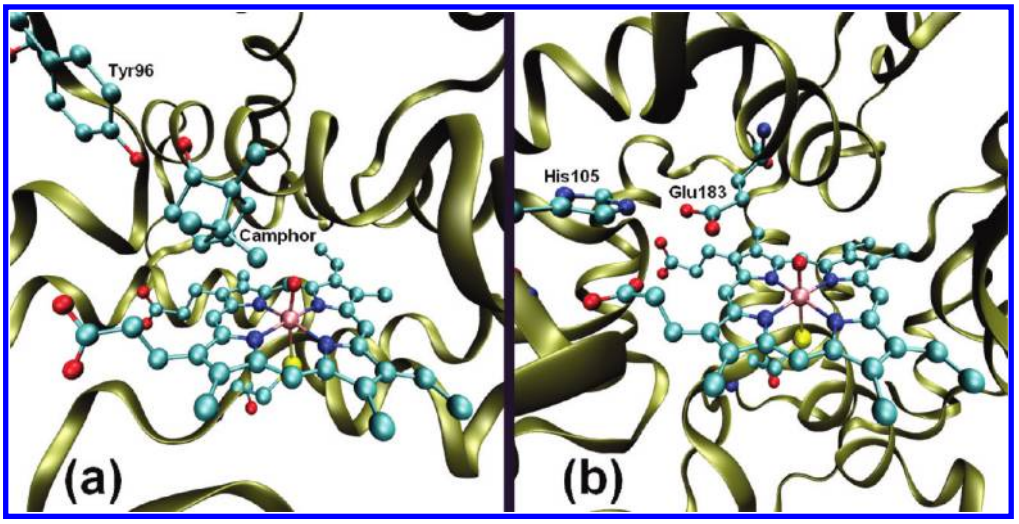


**Figure 2.** (a) P450cam Cpd I[142] and (b) CPO Cpd I.[71]

since sulfur-based radicaloid states could be low lying in Cpd I, studying them by including sulfur-based orbitals in the active space should be necessary. Furthermore, as argued in the previous sections, inclusion of the double-shell effect in the active space is essential for the accuracy of the calculations. Finally, knowing the sensitivity of the electronic structure of Cpd I to the environment,[138−141] reliable results require actually CASPT2/MM calculations.

Based on the above insight, the present authors[132] recently studied the Cpd I species of the cysteine ligated heme enzymes, P450cam and chloroperoxidase (CPO), using QM(CD-CASPT2)/MM calculations. These Cpd I species in their protein environments are shown in Figure 2.

This study aimed at providing a more complete picture of low-lying states of Cpd I in these enzymes by using a well-balanced active space based on the above guidelines. Of special interest were the spin states that are obtained by ferromagnetic and antiferromagnetic coupling of $Por^{\bullet+}$ ($S = {}^1/_2$, with $a_{2u}$ singly occupied) with Fe(IV)═O ($S = 1$ and 2) leading to the ${}^{2S+1}A_{2u}$ states with $S = {}^1/_2$ and ${}^3/_2$; most of these states are triradicaloids, while one is pentaradicaloid. In addition, the relative energy of the $A_{1u}$ state (with $a_{1u}$ singly occupied) had to be settled. Finally, it was deemed necessary to ascertain the relative energy of the Fe(V)═O states ($S = {}^1/_2;{}^3/_2$), which involve a closed-shell porphyrin and a $d^3$ iron configuration, which have been repeatedly invoked as the reactive states of P450.[143,144] To achieve this, all low-lying states, of various iron configurations within the iron 3d shell and the ligands, up to about 30 kcal/mol from ground state were explored. In some cases (see later), it was necessary to carry out state specific CASPT2 calculations, rather than state-average calculations.

Geometries of the two Cpd I species were optimized without symmetry constraints at a similar level to the one used by Neese and Thiel et al.[135,136] To reduce the systematic error of CASPT2 in state gap calculations involving different numbers of unpaired electrons, the standard IPEA-shifted zero-order Hamiltonian was used. The employed basis set was extended to the state-of-the-art level by using a multiple polarized triple-ζ quality for iron and its first coordinate sphere and a polarized double-ζ quality for the rest of the atoms. Scalar relativistic effects were accounted for by second-order DKH transformation,[120] and the 3s3p correlation

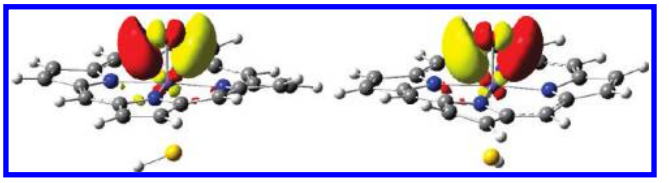

**Figure 3.** Two perpendicular iron $4d_{yz}$ and $4d_{xz}$ orbibals that mixed strongly with corresponding oxo O 3p orbitals in Cpd I.

effect in CASPT2 calculation was treated with a basis set optimized for iron semicore valence correlation (cc-pwCVTZ).[145] The active space included the relevant $\pi$-type orbitals of porphine ($a_{1u}$ and $a_{2u}$) and four pairs of bonding/antibonding orbitals between the iron 3d shell and surrounding ligands, as done before.[136] In addition, $3d_{xy}$ (iron 3d nonbonding), sulfur-based orbitals, $4d_{xy}$, and two other 4d orbitals ($4d_{yz}$ and $4d_{xz}$) for the double-shell effect were included. As shown in Figure 3, the latter two 4d orbitals mix strongly with O 3p orbtials due to the strong covalent character of the Fe═O bond in the high-valent iron-oxo system, which does not exist in other heme species.

The main results of this study[132] for Cpd I can be summarized as follows:

(1) At the CASPT2 level, the $A_{1u}$ states in P450cam Cpd I lie 18−19 kcal/mol higher than the corresponding $A_{2u}$ states. This result is comparable to the TDDFT/MM data (12.3 kcal/mol),[136] and gas-phase CASPT2 results (22−25 kcal/mol),[137] but significantly larger than the DDCI2+Q/MM result (1.9 kcal/mol).[136] This result is also more consistent with the previous CASPT2 calculation for $A_{1u}/A_{2u}$ state splitting in the $PorFeF_2$ (13−18 kcal/mol) system.[129] As found before in Cpd I[136,137] and also in other heme systems,[127] using CASSCF, which considers only nondynamic correlation, yields an $A_{1u}$ below $A_{2u}$ state ordering. Thus, it is the dynamic correlation that reverses this state level ordering.

(2) The pentaradicaloid state ${}^4A_{2u}$ arises from the corresponding ${}^2A_{2u}$ triradicaloid state by one-electron excitation out of $3d_{xy}$ to $3d_{x^2-y^2}$ (see the orbital diagram in Scheme 4). In the absence of the double-shell effect, the pentaradicaloid state in P450cam is 5.4 kcal/mol more stable than the triradicaloid state. However, the double-shell effect of the

$4d_{xy}$ orbital favors by 3.5 kcal/mol the triradicaloid state, which possesses a doubly occupied $3d_{xy}$ orbital. This finding may well be relevant to other high-valent nonheme iron-oxo species.[135]

(3) Despite this double-shell effect, CASPT2/MM predicts that the pentaradicaloid and triradicaloid states should be virtually degenerate. However, as we noted above, CASPT2 tends to overestimate the stability of states with more unpaired electrons for some heme systems (see the discussions of the Fe(II) systems in sections i and ii). Apparently, it is quite possible that the standard IPEA-shifted zero-order Hamiltonian still does not fully remedy this bias in the case of the high-valent iron(IV)-oxo system. The overestimation of the stability of the pentaradicaloid state may be as much as 5−10 kcal/mol, as noted by Pierloot and Radoń et al. for the Fe(II) state.[119,122] In addition, due to the error limit of the CASPT2 method (4−7 kcal/mol), accurate determination of these gaps is still difficult. The B3LYP/MM gap of 12 kcal/mol is on the higher side, but it may after all turn to be not a bad estimate.

(4) The doublet and quartet Fe(V) states were calculated to be low-lying exited states, within 10 kcal/mol from the ground triradicaloid state.

(5) The sulfur-based radicaloid states are quite high lying in P450cam (around 30 kcal/mol) and could be safely excluded from the scope of mechanistic exploration for P450 enzymes.

In addition to the above results, some specific new experience was gained in this work about the usage of CASPT2 calculation for transition-metal-containing systems. Thus, there is a tendency to prefer state-average calculations that presumably handle all states on equal footing. However, as noted by the present authors,[132] for states that involve different metal oxidation numbers, the metal d orbitals could be quite different due to different screening of the Fe atom at different oxidation states, for example, for the Fe(V) vs the Fe(IV) states. This significant difference makes the state-average calculation, in fact, less of equal footing for the calculated states, especially when the numbers of the states having different oxidation states are different in the state-average CASSCF calculation. A typical problem of this kind was noted for the energy difference of the Fe(V)/Fe(IV) states in Cpd I. Thus, using the state-average CASSCF reference places the PorFe(V)=O states even lower than the $Por^{\bullet+}$Fe(IV)=O states at the CASPT2 level, which is in contrast to the experimental result for CPO Cpd I, wherein the ground state is definitely $Por^{\bullet+}$Fe(IV)=O. This artificial lowering originates in the orbital-occupancy differences, which make the state-average CASSCF reference less appropriate for the Fe(V) states compared with the Fe(IV) states. This in turn leads to relatively larger perturbation in the CASPT2 calculation for the Fe(V) states, and hence an overestimated dynamic correlation energy. We note that problems due to different oxidation states only exist in systems with noninnocent ligands, which can donate/accept one electron to/from the transition metal center, thus changing its the oxidation state. Another lesson from the above analysis is the recognition that TDDFT, which lacks orbital relaxation,[146] will place the energy of the Fe(V) state much too high relative to the ground Fe(IV) state.

Although we do not recommend state-average CASSCF calculations for states having different metal oxidation states, when the target state is a high-energy root in CASSCF calculation, then state-average calculation becomes indispensable. This in turn shows that CASPT2 still does not have a canonical procedure that can generate automatically relative state energies in complex situations like Cpd I. Thus, all the above findings, notably the relative energies of the Fe(V) states and pentaradicaloid Fe(IV) state, reflect the difficulties inherent in MR/MC calculations and must await future testing.

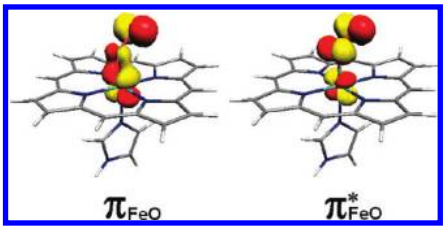


**Figure 4.** The two MOs which are alternately doubly occupied/vacant in the two dominant CASSCF configurations, i.e., $|...\pi_{FeO}{}^2\rangle$ and $|...\pi^*_{FeO}{}^2\rangle$.

**iv. Hexa-Coordinate Heme with Diatomic Molecule or Triatomic Molecule as the Sixth Ligand.** Diatomic molecules such as $O_2$, NO, and CO are ligated by heme protein enzymes and are used in processes of bond activation, transport, storage, and sensing.[147] The following subsections describe the MR/MC calculations of some of these complexes.

*Oxy−Heme Complexes.* The dioxygen molecule is one of the biologically most important ligands for heme enzymes, which either reduce it to form the active species Cpd I as in P450 or transport it to vital tissues as in myoglobin (Mb) or hemoglobin (Hb), etc. The interest in $O_2$ coordinated heme (oxy-heme) has a long history dating back to the 17th century with the discovery of John Mayow who described the conversion of venous blood to arterial blood in the presence of air and/or *Saltpeter* ($KNO_3$). In 1936, Pauling showed that the paramagnetic ferrous deoxyheme ($S = 2$) form of Hb is converted in the presence of $O_2$ to oxy-Hb,[148] which is diamagnetic. To account for the dramatic spin change, Pauling suggested a bonding model for oxy-Hb, wherein both the ferrous and $O_2$ moieties were combined in their singlet states ($S_{Fe(II)}=0/S_{O_2}=0$) and were bonded via a coordinative Fe−$O_2$ bond. This model has started a debate on the nature of the Fe−$O_2$ bond, leading to at least two more models and many heated discussions that have been described recently.[149] One of these models is the Weiss superoxo model,[150] in which the Fe(II) moiety transfers an electron to $O_2$, and the so resulting Fe(III) and $O_2^-$ then bind. The second is the McClure−Goddard model,[80,81,151] wherein the two neutral moieties combine in their triplet states ($S_{Fe(II)}=1/S_{O_2}=1$) and are doubly bonded.

Early on, it was concluded that this bonding mechanism cannot be described by a single determinant and it requires MR/MC computations. This has led to a few early ab initio MC studies. Thus, in 1989 and 1993, Yamamoto and Kashiwagi[152,153] published two papers on their CASSCF calculations of the ground state of the oxyheme system. The model system used is initially $O_2$FePorNH$_3$, and later the $NH_3$ was replaced by an imidazole (Im) ligand. The geometries of the complexes were constructed from the experimentally determined systems of related synthetic models. The active space (14,11) was comprised of five iron 3d orbitals and six valence bonding/antibonding orbitals of the O−O moiety. The CASSCF calculations predicted a singlet ground state, and had a wave function dominated by two closed-shell configurations (77−78% weight in total), which differed in the occupancy of the orbitals in

Figure 4, i.e., $|...\pi_{FeO}{}^2\rangle$ and $|...\pi^*_{FeO}{}^2\rangle$, with a larger weight of the former.

Although these early calculations involved small basis sets, the dominance of the two configurations in Figure 4 has characterized all the subsequent MC calculations of oxyheme, but their significance became clear only recently.[149] Initially, Kashiwagi et al. took their CASSCF result as support for the Pauling bonding model ($S_{Fe(II)}=0/S_{O_2}=0$)[152] but shifted later[153] to support the McClure−Goddard doubly bonded model. In a letter, Harcourt[154] considered the first CASSCF result of Kashiwagi et al.,[152] and showed us that using MO configurations to distinguish between the bonding models of Pauling, Weiss, and McClure−Goddard is not straightforward because those bonding models are all based on valence bond (VB) structures and not on MO configurations. Harcourt's comment went however unnoticed.

In 2005, Jensen et al. published the first CASPT2 study for the $O_2$FePorIm system,[155] using a BP86 optimized geometry with $C_s$ symmetry constraint. The CASPT2 study employed a (14,13) active space, which included in addition to the five 3d orbitals and $O_2$ $\pi$-type orbitals also three 4d virtual orbitals, for double-shell effects, and one Fe−N equatorial bonding orbital. A large ANO basis set was used on iron and its immediate coordinate sphere. Similar to previous results,[152,153] two configurations were found to be dominant (more than 80% in weight) in the CASSCF wave function for the lowest singlet state. However, at the CASPT2 level, the triplet state was found to be the ground state (2.8 kcal/mol lower than the singlet state), which is in contrast to the experimental consensus that the singlet state is the ground state of oxyheme, indicating that generating a singlet ground state is not a trivial task for CASPT2 calculation. Initially, Jensen et al. concluded that Pauling bonding is dominant but later revised their conclusion, arguing that a picture blending the Pauling, Weiss, and McClure−Goddard bonding models was more appropriate.

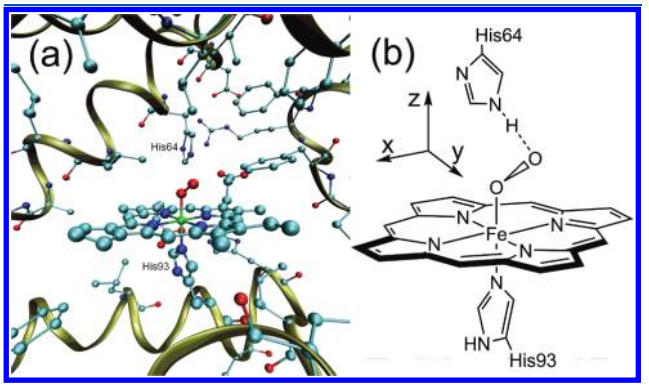


**Figure 5.** (a) The active site of oxy-Mb (PDB code 2ZS6).[60] (b) The QM region in QM/MM calculations.[149]

Novoa et al.[156] used the CASPT2 method to explore the energy profile during the $O_2$ binding to ferrous heme, using $O_2$FePorIm as the ferrous model, and the BP86/SVP optimized geometry (with $C_s$ constraint). Compared with Jensen et al.,[155] Novoa et al. used a larger basis set for Fe and O and a smaller one for N. The active space (16,14) included now also the O−O $\sigma$/$\sigma^*$ orbitals, whereas $4d_{yz}$ was not included. The key results of this study can be summarized as follows:

(1) The CASPT2 method provides a good quantitative description of the $O_2$ binding process to the Fe(II) center, which is shown to involve triplet, quintet, and heptet states through van der Waals intermediates with longer Fe−$O_2$ bond distances. These van der Waals minima were expectedly absent in the previous DFT studies.[157−159]

(2) Unlike the previous CASPT2 calculation,[155] at the geometry of the singlet state ($R_{Fe-O} \approx 1.8$ Å), the singlet oxyheme is calculated to be the ground state with CASPT2. However, the triplet state is found to be the global minimum with a longer Fe−O distance ($R_{Fe-O} \approx 2.6$ Å) than the singlet local minimum. It should be noted that the triplet state of oxy-heme could be overstabilized in the absence of the protein environment of Mb.[149]

To resolve the Fe−$O_2$ bonding nature and explore the protein environment effect on its description, the Jerusalem group[149] studied recently the oxy-Mb complex, shown in Figure 5, using QM(CASSCF)/MM calculations.

On the basis of the protein environment (see Figure 5a), the choice QM region was $Im_{64}/O_2FePorIm_{93}$, where $Im_{64}$ is the imidazole ring of distal histidine His64 (E7) that participates in H-bonding to the O−O moiety of oxyheme, in Figure 5b, whereas $Im_{93}$ is the axial ligand bound to iron via the imidazole ring of proximal histidine His93 (F8). To distinguish the protein effect from the intrinsic properties of the oxy-heme, an $O_2$FePorIm model was studied by means of CASSCF-only gas-phase calculations. The geometry was optimized at the B3LYP/MM level without any symmetry constraints. A basis set of similar

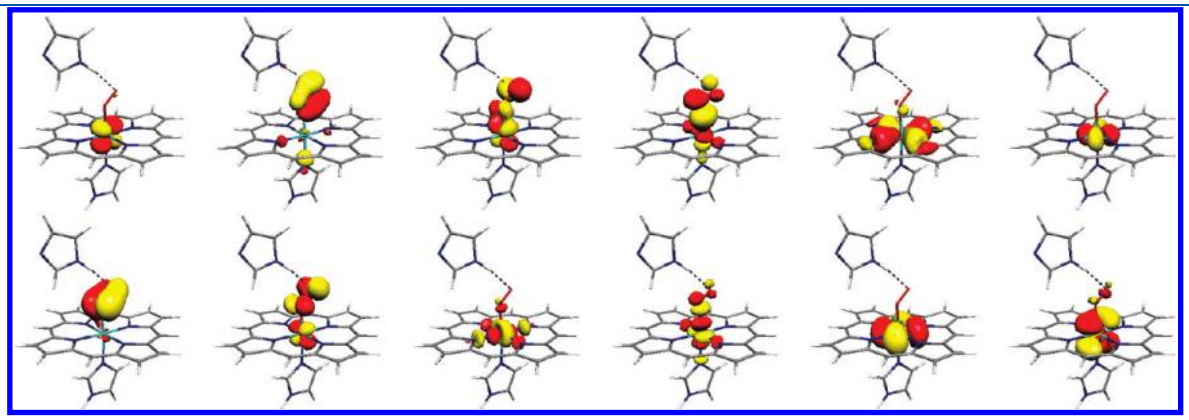

**Figure 6.** The active space used in CASSCF/MM calculation for oxy-Mb. Reprinted with permission from ref 149. Copyright 2008 American Chemical Society.

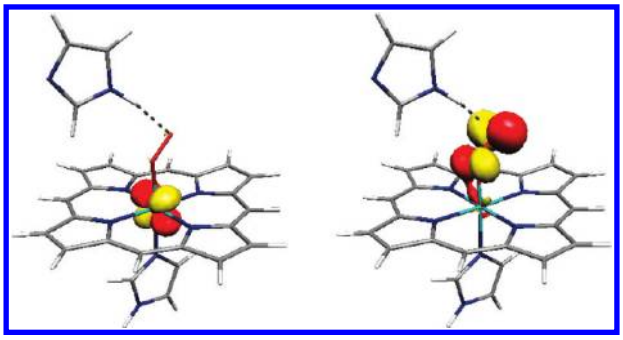

**Figure 7.** The two GVB singlet-paired orbitals obtained by orbital transformation from the two dominant configurations in the CASSCF/MM wave function of oxy-Mb. Reprinted with permission from ref 149. Copyright 2008 American Chemical Society.

quality to previous studies,[155,156] was used for the CASSCF calculation. The active space (14,12) used is almost the same as the one used by Jensen et al.,[155] except for the removal of $4d_{yz}$ (see Figure 6), as done in Novoa's CASPT2 work.[156] The main results of this study are the following:

(1) The bulk polarity of the protein and the H-bond donation by the distal His64 residue exert a strong effect on the electronic structure of the oxy-heme complex, on the relative energies of the spin states ($S$ = 0 and 1), and on the charge distribution of the $O_2$ moiety. The protein polarizes the Fe−O and weakens its $\pi$-bonding component. Additionally, compared with the CASSCF/MM calculations, the gas-phase CASSCF calculations gave different state ordering of the two lowest lying triplet states and different relative energy gaps above the singlet ground state. These differences emphasize the fact that gas-phase MR/MC results must be considered with caution.

(2) As already pointed out, the CASSCF wave function of the singlet ground state is dominated by the two configurations, one with a doubly occupied $\pi_{FeO}$ and the other with a doubly occupied $\pi^*_{FeO}$ (see Figure 4). This dominance is more pronounced in the CASSCF/MM calculation (~90% in weight) compared with the gas phase (~79% in weight). This configuration content of the wave function enabled us to perform an orbital transformation that converts $\Psi_{CASSCF}$ to a $\Psi_{GVB}$-type wave function, wherein the two orbitals in Figure 7 are spin-paired into a singlet bond pair. The transformed orbitals in Figure 7 have dominant iron $3d_{yz}$ and $\pi_{\perp}^*$(O−O) characters, with some delocalization tails. As such, the CASSCF/MM wave function corresponds to an antiferromagnetic coupling of the odd electron in Fe(III) and $O_2^-$, respectively, which is in fact very much like the Weiss model.[150]

(3) The so transformed CASSCF/MM wave function *is virtually identical to the symmetry broken DFT/MM description of the oxy-heme species*.[149] In fact, one can use the natural Kohn−Sham orbital population to reconstruct a CASSCF-type wave function from the DFT/MM results. The CASSCF-only wave function in the gas phase is similar; however, the transformed orbitals have large delocalization tails, and hence correspond to a more covalent $\pi$-bonding between the Fe(III) and $O_2^-$ moieties.

The recent study of Radoń and Pierloot[119] used CASPT2 and several popular density functionals to address the binding energies of XO (X = C, O, N) with heme model systems Fe(II)PorIm and Fe(II)Por. The authors showed that, unlike most popular functionals (with the exception of OLYP), CASPT2 predicts correct Fe−$O_2$ binding energies (with a (16,14) active space). However, as has been argued by Siegbahn,[160] adding empirical dispersion correction to B3LYP produces reasonably good Fe−$O_2$ binding energies.

*CO− and NO−Heme Complexes.* CO is an important ligand serving as a spectroscopic probe in those heme proteins/enzymes.[161] However, it is also implicated as a diffusive neurotransmitter that is formed during heme catabolism by heme oxygenase.[162−166] Biological NO is formed by the enzyme nitric oxide synthase,[167] and its ligation to iron constitutes a signaling event in biological processes.[168]

Compared with Fe−NO bonding, the Fe(II)−CO complexation is simple and it usually leads to low spin closed-shell ground states due to the strong ligand field of CO. However, the NO coordination to heme adds an odd electron to the complex. This creates some ambiguity on the oxidation state assignment and the electron count of Fe−NO complexes, and hence one uses the Enemark−Feltham electron count notation,[169] which sums the odd electron of NO into the d-count. In this notation, an Fe(II)−NO complex would be labeled as $\{FeNO\}^7$, wherein the superscript sums the ferrous iron six 3d electrons and the odd electron brought by NO. This notation however still does not disclose either the contributing oxidation states or the Fe−NO bonding type. Thus, understanding the binding mode of NO with heme is quite intriguing.

Recently, Radoń and Pierloot[119] published a systematic study on the binding energies of XO (X = O, C, N) with Fe(II)PorIm and Fe(II)Por, using CASPT2 and several popular density functionals. Since their study of the Fe−$O_2$ complex was mentioned above, here we discuss only the latter two complexes, and only for the (XO)Fe(II)PorIm systems.

The CASPT2 calculations were performed on PBE0 or BP86 geometries, and involved basis sets up to multiple polarized quadruple-ζ quality for iron and (multiple) polarized triple-ζ quality for the first coordinate sphere of iron. For (XO)Fe(II)-PorIm, the active spaces used are (16,15) and (15,14) for CO and NO, respectively. Because of the linear Fe−CO moiety, the active space for the Fe−CO complex contained also the carbon lone orbital pointing toward Fe. The main finding is that CASPT2 combined with a relatively large basis set leads to binding energies of XO molecules to heme in satisfactory agreement with experimental data derived from Mb; the CASPT2 underbinding is only up to 1.1 kcal/mol. However, considering basis-set incompleteness and the systematic error found for the pentacoordinate XOFe(II)PorIm complexes, the authors expressed their opinion that the good agreement with experiment is due to error cancellation.

In a subsequent work,[170] Radoń et al. performed a detailed CASPT2 study of the Fe(II)−NO bonding in the doublet and quartet states (see Scheme 7) of several heme and nonheme systems, using BP86/def2-TZVP geometries. The CASPT2 calculations involved basis sets similar to the previous work.[119] The active space (11,14) used for the quartet state of (NO)Fe(II)PorIm and (NO)Fe(II)Por$NH_3$ differs a bit from the previously used one, (15,14), by replacing two occupied NO $\pi$ bonding orbitals with two virtual $4d_{xy}$ and $4d_{z^2}$ orbitals (see

**Scheme 7. Orbital Occupancy Diagrams for the Doublet and Quartet States of the Hexa-Coordinate Fe(II)-Nitrosyl Heme System**[170]

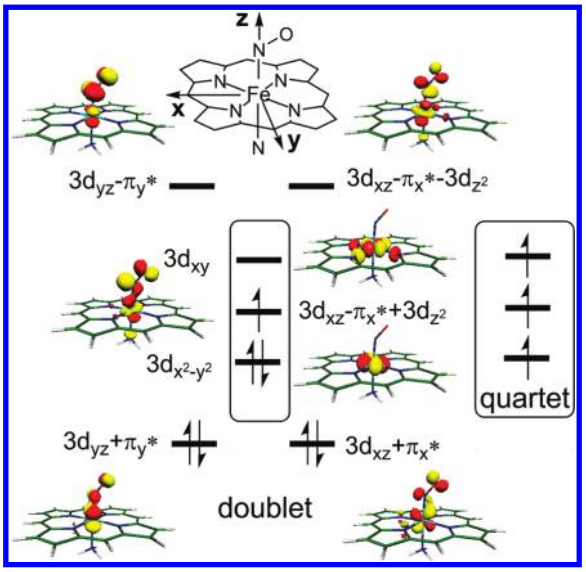


Scheme 7 for Cartesian coordinates) and replacing the $Fe-N_{axial}$ $\sigma$ bonding orbital with the $Fe-N_{NO}$ $\sigma$ bonding orbital. The $Fe-N_{axial}$ $\sigma$ bonding orbital is removed because previously it was found that this orbital could not be kept in active space simultaneously with $4d_{z^2}$.[119] For the doublet state, where $3d_{xy}$ is empty (Scheme 7), the active space was decreased to (11,13) by removing the corresponding $4d_{xy}$ orbital.

Radoń et al. analyzed the complex CASSCF wave function using orbital localization. In the new localized-orbital basis, the CASSCF wave function was found to exhibit antiferromagnetic coupling interactions between the fragment−orbital pairs $3d_{yz}/\pi_y^*$ and $3d_{xz}/\pi_x^*$. These antiferromagnetic couplings originated from the localization of the bonding−antibonding orbitals $3d_{yz} \pm \pi_y^*$ and bonding−nonbonding−antibonding orbitals $3d_{xz} \pm \pi_x^* \pm d_{z^2}$ shown in Scheme 7. We note that the antiferromagnetic coupling corresponding to the $3d_{yz} \pm \pi_y^*$ pair is quite similar to the above-mentioned CASSCF → GVB transformation of the oxy-Mb system.[149]

The other interesting results of this work were the following:

(1) Contrary to a previous suggestion,[119] $Fe^{I}-NO^{+}$ was not found to be the predominant VB configuration in bonding mode between Fe(II) and NO. The predominant VB-type configurations were found to be $Fe^{II}-NO^{0}$ and $Fe^{III}-NO^{-}$. These configurations emphasize the weakness of the oxidation-state formalism for specifying the actual oxidation states in nitrosyl complexes.

(2) As had been found previously,[119] here too the CASSCF spin density was consistent with pure functionals like BP86 and OLYP, and less so with hybrid functionals like B3LYP and B3LYP*, in accord with previous findings.[171] Nevertheless, as noted by the authors,[170] in agreement with two of us,[149] DFT methods are trying to mimic the results of MR calculations.

(3) Systematic errors are likely to exist in the CASPT2 calculated doublet−quartet energy gaps due to $3d_{x^2-y^2} \rightarrow 3d_{xy}$ promotion (see Scheme 7).

## CONCLUSIONS

In this review, we have discussed recent theoretical studies for heme-related systems by ab initio multireference/multiconfiguration (MR/MC) methods. The calculations have been met so far with reasonable success and have shed light on otherwise more complex and difficult electronic structure problems of heme-related systems. However, the MR/MC methods have also problems and limitations. With particular emphasis on the latter aspect, we summarize herein our most important conclusions from these studies:

(1) A balanced treatment of the ground state and excited states is always very important in the MR/MC methods when dealing with more than one electronic state. As a consequence, the double-shell effect for the heme-related system appears to be crucial for spin-state energetics and ordering, which is by far the most common type of application of the ab initio MR/MC methods in these systems. Due to computational limitations and active-space stability issues, it is suggested to consider only those 4d orbitals corresponding to doubly occupied 3d.[172] The computational limitation may hopefully be eliminated by applying the RASPT2 (restricted active space SCF followed by PT2) method,[173] which enables one to use much larger active spaces than before while employing selectively chosen excitations within the orbital window. One is curious to see whether RASPT2 can indeed alleviate the uncertainty of CASPT2 regarding the identity of the ground state[132] for P450 Cpd I and reproduce the recent experimental results,[174] which show that the ground state is definitely the triradicaloid $^2A_{2u}$ state.

(2) For spin-state energetics and ordering of some heme systems like Fe(II)Por and PorFe(IV)-oxo (but not Fe(III)Por), which are characterized by the difference of $(d_{x^2-y^2})^1(d_{xy})^1/(d_{x^2-y^2})^0(d_{xy})^2$ configurations, even the standard IPEA-shifted zero-order Hamiltonian may still face systematic errors of CASPT2. Thus, more investigations are required for a clear assessment of the accuracy of CASPT2 for heme systems.

(3) Because heme species are quite relevant to many enzymatic systems, it is often necessary to include the protein environment. From the presently available results, the protein exerts two apparent effects: first, the electronic structure of heme systems, calculated with MR/MC methods, appears to be more sensitive to the presence or absence of the protein environment compared with DFT methods; second, the protein environment sometimes can eliminate difficulties which incur in gas-phase MR/MC calculations, as seen in the case of Cpd I.[132,137]

(4) Expanding the complex multiconfigurational wave function on localized orbitals, at least in the cases studied, provides insightful pictures of bonding in terms of contributing valence bond structures. At present, the localization can be done either with procedures[131,170,175] which keep the orthogonality of the localized orbitals or with some appropriate wave function transformations which produce effectively localized but non-orthogonal orbitals.[149] In the future, one might consider also localization procedures that map the CAS orbitals to some reference fragment orbitals,[176−181] followed by diagona-

lization within the new basis-orbital set. Be the localization method as it may, it simplifies the complex CI expansion and produces a lucid bonding mechanism.

Finally, although we have gone through many applications of ab initio MR/MC methods to heme systems, the main issue that has been addressed by the various studies is the relative energies of different spin states. It is expected that in the future this will be followed by other types of applications, such as calculations of kinetic parameters in chemical reactions, molecular properties, and molecular spectroscopy.[182] After all, for some of these types of applications, which only involve one electronic state, MR/MC methods could possibly achieve better accuracy than relative spin-state energies, which is indeed a difficult task whose accuracy requires a very balanced treatment of electron correlation for a few states. At present, this is still not always possible. In addition, since the MR/MC method does not suffer from spin contamination, it may also avoid the potential ambiguity between single reference coupled cluster methods based on symmetry broken vis-a-vis restricted open-shell wave functions, as observed e.g., in calculations of barriers for hydrogen abstraction by iron-oxo complexes,[183,184] which are typified by exchange-enhanced reactivity.[185]

## AUTHOR INFORMATION

### Corresponding Author

*Fax: +972 (0)2 658 4033. E-mail: chenh@yfaat.ch.huji.ac.il (H.C.); sason@yfaat.ch.huji.ac.il (S.S.).

## BIOGRAPHIES

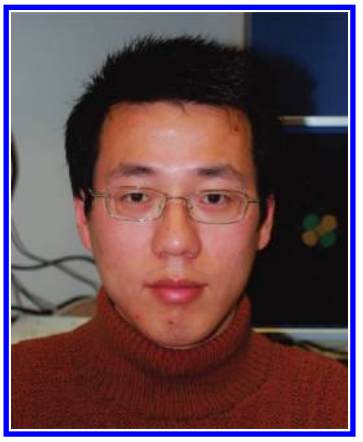

Hui Chen received his B.Sc. (2001) in chemistry and Ph.D. (2006) in physical chemistry both from Nanjing University (China), under the supervision of Prof. Shuhua Li in Institute of Theoretical and Computational Chemistry, with work on the theoretical studies of photochemistry and photophysics of organic molecules. Then, he worked with Prof. Sason Shaik at the Hebrew University as a postdoctoral fellow until now. He is the recipient of a Golda Meir Fellowship (2007−2009) and won the Lise Meitner Prize of the Lise-Meitner-Minerva Center (2007) for computational quantum chemistry. In April of 2011, he will join Institute of Chemistry, Chinese Academy of Sciences (CAS), to become a faculty member there. His current main research interests are in theoretical study of the intriguing reaction mechanism and electronic structure problem in complex chemical and biochemical systems.

Wenzhen Lai received her B.Sc. (2002) in chemistry from Sichuan University (China). Under the supervision of Prof. Daiqian Xie, she obtained her M.Sc. (2005) in physical chemistry from Sichuan University and Ph.D. (2008) in theoretical and computational chemistry from Nanjing University (China) conducting theoretical research on heterogeneous catalytic reactions on transition metal surfaces and photodissociation of small molecules. Now, she is a postdoctoral fellow with Prof. Sason Shaik at the Hebrew University. Her current major interests involve metallo-enzymes and their model systems and catalysis mechanisms.

Sason Shaik has received his B.Sc. and M.Sc. in chemistry from Bar-Ilan University and his Ph.D from the University of Washington under Nicholaos D. Epiotis. In 1978/9, he spent a Post Doctoral year with Roald Hoffmann at Cornell University. In 1980, he started his first academic position as a Lecturer at Ben-Gurion University where he became Professor in 1988. In 1992, he moved to the Hebrew University, where he is currently the director of The Lise Meitner-Minerva Center for Computational Quantum Chemistry. Among the awards he received are the Lise-Meitner-Alexander von Humboldt Senior Award in 1996−1999, the 2001 Israel Chemical Society Prize, the 2001 Kolthoff Award, and the 2006 Schrödinger Medal. He is an AAAS fellow and a WATOC fellow. His research interests are in the use of quantum chemistry, and in particular of valence bond theory, to develop paradigms which can pattern data and lead to the generation and solution of new problems. He started his P450 and heme research in 1998 and has been fascinated ever since!

## ■ ACKNOWLEDGMENT

S.S. is supported by an ISF grant (53/09). In memoriam of Prof. Björn O. Roos, who has contributed so much to ab initio quantum chemistry.

## ■ REFERENCES

(1) Poulos, T. L. In *The Porphyrin Handbook*; Kadish, K. M., Smith, K. M., Guilard, R., Eds.; Academic Press: San Diego, CA, 2000; Vol. 4, Chapter 32, pp 189−218.
(2) Shaik, S.; Kumar, D.; de Visser, S. P.; Altun, A.; Thiel, W. *Chem. Rev.* **2005**, *105*, 2279–2328.
(3) Shaik, S.; Hirao, H.; Kumar, D. *Acc. Chem. Res.* **2007**, *40*, 532–542.
(4) Shaik, S.; Hirao, H.; Kumar, D. *Nat. Prod. Rep.* **2007**, *24*, 533–552.
(5) Shaik, S.; de Visser, S. P.; Kumar, D. *J. Biol. Inorg. Chem.* **2004**, *9*, 661–668.
(6) Ghosh, A.; Steene, E. *J. Biol. Inorg. Chem.* **2001**, *6*, 739–752.
(7) Ghosh, A. *J. Biol. Inorg. Chem.* **2006**, *11*, 712–724.
(8) Ghosh, A. *Acc. Chem. Res.* **2005**, *38*, 943–954.
(9) Siegbahn, P. E. M.; Blomberg, M. R. A. *Chem. Rev.* **2000**, *100*, 421–437.
(10) Himo, F.; Siegbahn, P. E. M. *Chem. Rev.* **2003**, *103*, 2421–2456.
(11) Siegbahn, P. E. M.; Borowski, T. *Acc. Chem. Res.* **2006**, *39*, 729–738.
(12) Bassan, A.; Blomberg, M. R. A.; Borowski, T.; Siegbahn, P. E. M. *J. Inorg. Biochem.* **2006**, *100*, 727–743.
(13) Spiro, T. G.; Zgierski, M. Z.; Kozlowski, P. M. *Coord. Chem. Rev.* **2001**, *219*, 923–936.
(14) Spiro, T. G.; Jarzecki, A. A. *Curr. Opin. Chem. Biol.* **2001**, *5*, 715–723.
(15) Hersleth, H. P.; Ryde, U.; Rydberg, P.; Görbitz, C. H.; Andersson, K. K. *J. Inorg. Biochem.* **2006**, *100*, 460–476.
(16) Yoshizawa, K. *Coord. Chem. Rev.* **2002**, *226*, 251–259.
(17) Degtyarenko, I.; Biarnés, X.; Nieminen, R. M.; Rovira, C. *Coord. Chem. Rev.* **2008**, *252*, 1497–1513.
(18) Bikiel, D. E.; Boechi, L.; Capece, L.; Crespo, A.; De Biase, P. M.; Di Lella, S.; González Lebrero, M. C.; Martí, M. A.; Nadra, A. D.; Perissinotti, L. L.; Scherlis, D. A.; Estrin, D. A. *Phys. Chem. Chem. Phys.* **2006**, *8*, 5611–5628.
(19) Senn, H. M.; Thiel, W. *Curr. Opin. Chem. Biol.* **2007**, *11*, 182–187.
(20) Senn, H. M.; Thiel, W. *Top. Curr. Chem.* **2007**, *268*, 173–290.
(21) Senn, H. M.; Thiel, W. *Angew. Chem., Int. Ed.* **2009**, *48*, 1198–1229.
(22) Ryde, U. *Curr. Opin. Chem. Biol.* **2003**, *7*, 136–142.
(23) Friesner, R. A.; Guallar, V. *Annu. Rev. Phys. Chem.* **2005**, *56*, 389–427.
(24) Lin, H.; Truhlar, D. G. *Theor. Chem. Acc.* **2007**, *117*, 185–199.
(25) Hu, H.; Yang, W. T. *Annu. Rev. Phys. Chem.* **2008**, *59*, 573–601.
(26) Acevedo, O.; Jorgensen, W. L. *Acc. Chem. Res.* **2010**, *43*, 142–151.
(27) Ranaghan, K. E.; Mulholland, A. J. *Int. Rev. Phys. Chem.* **2010**, *29*, 365–133.
(28) Riccardi, D.; Schaefer, P.; Yang, Y.; Yu, H. B.; Ghosh, N.; Prat-Resina, X.; König, P.; Li, G. H.; Xu, D. G.; Guo, H.; Elstner, M.; Cui, Q. *J. Phys. Chem. B* **2006**, *110*, 6458–6469.
(29) Zhang, R.; Lev, B.; Cuervo, J. E.; Noskov, S. Y.; Salahub, D. R. *Adv. Quantum Chem.* **2010**, *59*, 353–400.
(30) See the recent review and many references therein for QM/MM studies of P450 enzymes: Shaik, S.; Cohen, S.; Wang, Y.; Chen, H.; Kumar, D.; Thiel, W. *Chem. Rev.* **2010**, *110*, 949–1017.
(31) Harvey, J. N.; Bathelt, C. M.; Mulholland, A. J. *J. Comput. Chem.* **2006**, *27*, 1352–1362.
(32) Bathelt, C. M.; Mulholland, A. J.; Harvey, J. N. *Dalton Trans.* **2005**, 3470–3476.
(33) Guallar, V.; Olsen, B. *J. Inorg. Biochem.* **2006**, *100*, 755–760.
(34) Guallar, V. *J. Phys. Chem. B* **2008**, *112*, 13460–13464.
(35) Heimdal, J.; Rydberg, P.; Ryde, U. *J. Phys. Chem. B* **2008**, *112*, 2501–2510.
(36) Alfonso-Prieto, M.; Borovik, A.; Carpena, X.; Murshudov, G.; Melik-Adamyan, W.; Fita, I.; Rovira, C.; Loewen, P. C. *J. Am. Chem. Soc.* **2007**, *129*, 4193–4205.
(37) Vidossich, P.; Alfonso-Prieto, M.; Carpena, X.; Loewen, P. C.; Fita, I.; Rovira, C. *J. Am. Chem. Soc.* **2007**, *129*, 13436–13446.
(38) Alfonso-Prieto, M.; Biarnés, X.; Carpena, X.; Vidossich, P.; Rovira, C. *J. Am. Chem. Soc.* **2009**, *131*, 11751–11761.
(39) Guallar, V.; Wallrapp, F. H. *Biophys. Chem.* **2010**, *149*, 1–11.
(40) Derat, E.; Cohen, S.; Shaik, S.; Altun, A.; Thiel, W. *J. Am. Chem. Soc.* **2005**, *127*, 13611–13621.
(41) Derat, E.; Shaik, S. *J. Am. Chem. Soc.* **2006**, *128*, 8185–8198.
(42) Derat, E.; Shaik, S. *J. Am. Chem. Soc.* **2006**, *128*, 13940–13949.
(43) Derat, E.; Shaik, S. *J. Phys. Chem. B* **2006**, *110*, 10526–10533.
(44) Derat, E.; Shaik, S.; Rovira, C.; Vidossich, P.; Alfonso-Prieto, M. *J. Am. Chem. Soc.* **2007**, *129*, 6346–6347.
(45) Vidossich, P; Fiorin, G; Alfonso-Prieto, M; Derat, E; Shaik, S; Rovira, C. *J. Phys. Chem. B* **2010**, *114*, 5161–5169.
(46) Zazza, C.; Amadei, A.; Palma, A.; Sanna, N.; Tatoli, S.; Aschi, M. *J. Phys. Chem. B* **2008**, *112*, 3184–3192.
(47) Zazza, C.; Palma, A.; Amadei, A.; Sanna, N.; Tatoli, S.; Aschi, M. *Faraday Discuss.* **2010**, *145*, 107–119.
(48) Fernández, M. L.; Martí, M. A.; Crespo, A.; Estrin, D. A. *J. Biol. Inorg. Chem.* **2005**, *10*, 595–604.
(49) Cho, K.-B.; Derat, E.; Shaik, S. *J. Am. Chem. Soc.* **2007**, *129*, 3182–3188.
(50) Cho, K.-B.; Carvajal, M. A.; Shaik, S. *J. Phys. Chem. B* **2009**, *113*, 336–346.
(51) de Visser, S. P. *Biochem. Soc. Trans.* **2009**, *37*, 373–377.
(52) Chen, H.; Moreau, Y.; Derat, E.; Shaik, S. *J. Am. Chem. Soc.* **2008**, *130*, 1953–1965.
(53) Lai, W. Z.; Chen, H.; Matsui, T.; Omori, K.; Unno, M.; Ikeda-Saito, M.; Shaik, S. *J. Am. Chem. Soc.* **2010**, *132*, 12960–12970.
(54) Rovira, C.; Schulze, B.; Eichinger, M.; Evanseck, J. D.; Parrinello, M. *Biophys. J.* **2001**, *81*, 435–445.
(55) Sigfridsson, E.; Ryde, U. *J. Inorg. Biochem.* **2002**, *91*, 101–115.
(56) Harvey, J. N. *Faraday Discuss.* **2004**, *127*, 165–177.
(57) Capece, L.; Martí, M. A.; Crespo, A.; Doctorovich, F.; Estrin, D. A. *J. Am. Chem. Soc.* **2006**, *128*, 12455–12461.
(58) Martí, M. A; Capece, L.; Bikiel, D. E.; Falcone, B.; Estrin, D. A. *Proteins* **2007**, *68*, 480–487.
(59) Freindorf, M.; Shao, Y. H.; Brown, S. T.; Kong, J.; Furlani, T. R. *Chem. Phys. Lett.* **2006**, *419*, 563–566.
(60) Unno, M.; Chen, H.; Kusama, S.; Shaik, S.; Ikeda-Saito, M. *J. Am. Chem. Soc.* **2007**, *129*, 13394–13395.
(61) Guallar, V.; Jarzecki, A. A.; Friesner, R. A.; Spiro, T. G. *J. Am. Chem. Soc.* **2006**, *128*, 5427–5435.
(62) Alcantara, R. E.; Xu, C.; Spiro, T. G.; Guallar, V. *Proc. Natl. Acad. Sci. U.S.A.* **2007**, *104*, 18451–18455.
(63) Perissinotti, L. L.; Martí, M. A.; Doctorovich, F.; Luque, F. J.; Estrin, D. A. *Biochemistry* **2008**, *47*, 9793–9802.
(64) Crespo, A.; Martí, M. A.; Kalko, S. G.; Morreale, A.; Orozco, M.; Gelpi, J. L.; Luque, F. J.; Estrin, D. A. *J. Am. Chem. Soc.* **2005**, *127*, 4433–4444.
(65) Martí, M. A.; Crespo, A.; Capece, L.; Boechi, L.; Bikiel, D. E.; Scherlis, D. A.; Estrin, D. A. *J. Inorg. Biochem.* **2006**, *100*, 761–770.
(66) Martí, M. A.; Bidon-Chanal, A.; Crespo, A.; Yeh, S. R.; Guallar, V.; Luque, F. J.; Estrin, D. A. *J. Am. Chem. Soc.* **2005**, *130*, 1688–1693.
(67) Guallar, V.; Lu, C. Y.; Borrelli, K.; Egawa, T.; Yeh, S. R. *J. Biol. Chem.* **2009**, *248*, 3106–3116.
(68) Kühnel, K.; Derat, E.; Terner, J.; Shaik, S.; Schlichting, I. *Proc. Natl. Acad. Sci. U.S.A.* **2007**, *104*, 99–104.
(69) Chen, H.; Hirao, H.; Derat, E.; Schlichting, I.; Shaik, S. *J. Phys. Chem. B* **2008**, *112*, 9490–9500.
(70) Lai, W. Z.; Chen, H.; Shaik, S. *J. Phys. Chem. B* **2009**, *113*, 7912–7917.

(71) Lai, W. Z.; Chen, H.; Cho, K.-B.; Shaik, S. *J. Phys. Chem. A* **2009**, *113*, 11763–11771.
(72) Lewis-Ballester, A.; Batabyal, D.; Egawa, T.; Lu, C. Y.; Lin, Y.; Marti, M. A.; Capece, L.; Estrin, D. A.; Yeh, S. R. *Proc. Natl. Acad. Sci. U.S.A.* **2009**, *106*, 17371–17376.
(73) Capece, L.; Lewis-Ballester, A.; Batabyal, D.; Russo, N. D.; Yeh, S. R.; Estrin, D. A.; Marti, M. A. *J. Biol. Inorg. Chem.* **2010**, *15*, 811–823.
(74) Chung, L. W.; Li, X.; Sugimoto, H.; Shiro, Y.; Morokuma, K. *J. Am. Chem. Soc.* **2010**, *132*, 11993–12005.
(75) Dedieu, A.; Rohmer, M. M.; Veillard, A. *Adv. Quantum Chem.* **1982**, *16*, 43–95.
(76) Edwards, W. D.; Weiner, B.; Zerner, M. C. *J. Am. Chem. Soc.* **1986**, *108*, 2196–2204.
(77) Herman, Z. S.; Loew, G. H. *J. Am. Chem. Soc.* **1980**, *102*, 1815–1821.
(78) Kuynh, B. H.; Case, D. A.; Karplus, M. *J. Am. Chem. Soc.* **1977**, *99*, 6103–6105.
(79) Case, D. A.; Kuynh, B. H.; Karplus, M. *J. Am. Chem. Soc.* **1979**, *101*, 4433–4453.
(80) Goddard, W. A., III; Olafson, B. D. *Proc. Natl. Acad. Sci. U.S.A.* **1975**, *72*, 2335–2339.
(81) Olafson, B. D.; Goddard, W. A., III. *Proc. Natl. Acad. Sci. U.S.A.* **1977**, *74*, 1315–1319.
(82) Rawlings, D. C.; Gouterman, M.; Davidson, E. R.; Feller, D. *Int. J. Quantum Chem.* **1985**, *28*, 773–796.
(83) Rohmer, M. M. *Chem. Phys. Lett.* **1985**, *116*, 44–49.
(84) Nakatsuji, H.; Hasegawa, J.; Ueda, H.; Hada, M. *Chem. Phys. Lett.* **1996**, *250*, 379–386.
(85) Nakatsuji, H.; Tokita, Y.; Hasegawa, J.; Hada, M. *Chem. Phys. Lett.* **1996**, *256*, 220–228.
(86) Tokita, Y.; Nakatsuji, H. *J. Phys. Chem. B* **1997**, *101*, 3281–3289.
(87) Miyahara, T.; Tokita, Y.; Nakatsuji, H. *J. Phys. Chem. B* **2001**, *105*, 7341–7352.
(88) Roos, B. O. *Adv. Chem. Phys.* **1987**, *69*, 399–445.
(89) Roos, B. O.; Andersson, K.; Fülscher, M. P.; Malmqvist, P. Å.; Serrano-Andrés, L.; Pierloot, K.; Merchán, M. *Adv. Chem. Phys.* **1996**, *93*, 219–331.
(90) Andersson, K.; Malmqvist, P. Å.; Roos, B. O.; Sadlej, A. J.; Wolinski, K. *J. Phys. Chem.* **1990**, *94*, 5483–5488.
(91) Andersson, K.; Malmqvist, P. Å.; Roos, B. O. *J. Chem. Phys.* **1992**, *96*, 1218–1226.
(92) Hirao, K. *Chem. Phys. Lett.* **1992**, *190*, 374–380.
(93) Hirao, K. *Chem. Phys. Lett.* **1992**, *196*, 397–403.
(94) Miralles, J.; Daudey, J. P.; Caballol, R. *Chem. Phys. Lett.* **1992**, *198*, 555–562.
(95) Miralles, J.; Castell, O.; Caballol, R.; Malrieu, J. P. *Chem. Phys.* **1993**, *172*, 33–43.
(96) Neese, F. *J. Chem. Phys.* **2003**, *119*, 9428–9443.
(97) Aquilante, F.; Malmqvist, P. Å.; Pedersen, T. B.; Ghosh, A.; Roos, B. O. *J. Chem. Theory Comput.* **2008**, *4*, 694–702.
(98) Ahlrichs, R.; Bär, M.; Baron, H. P.; Bauernschmitt, R.; Böcher, S.; Crawford, N.; Deglmann, P.; Ehrig, M.; Eichkorn, K.; Elliott, S.; Furche, F.; Haase, F.; Häser, M.; Horn, H.; Hättig, C.; Huber, C.; Huniar, U.; Kattcnnek, M.; Köhn, A.; Kölmel, C. Kollwitz, M.; May, K.; Nava, P.; Ochsenfeld, C.; Öhm, H.; Patzelt, H.; Rappoport, D.; Rubner, O.; Schäfer, A.; Schneider, U.; Sierka, M.; Treutler, O.; Unterreiner, B.; von Arnim, M.; Weigend, F.; Weis, P.; Weiss, H. *Turbomole-Program Package for ab initio Electronic Structure Calculations*, version 5.8; University of Karlsruhe: Karlsruhe, Germany, 2005.
(99) Neese, F. *ORCA-an ab initio, DFT and Semiempirical SCF-MO Package*, version 2.6; University of Bonn: Bonn, Germany, 2006.
(100) Aquilante, F.; de Vico, L.; Ferré, N.; Ghigo, G.; Malmqvist, P. Å.; Neogrády, P.; Pedersen, T. B.; Pitoňák, M.; Reiher, M.; Roos, B. O.; Serrano-Andrés, L.; Urban, M.; Veryazov, V.; Lindh, R. *J. Comput. Chem.* **2010**, *31*, 224–247.
(101) Andersson, K.; Roos, B. O. *Int. J. Quantum Chem.* **1993**, *45*, 591–607.
(102) Andersson, K. *Theor. Chem. Acc.* **1995**, *91*, 31–46.
(103) Ghigo, G.; Roos, B. O.; Malmqvist, P. Å. *Chem. Phys. Lett.* **2004**, *396*, 142–149.
(104) Karlström, G.; Lindh, R.; Malmqvist, P.-Å.; Roos, B. O.; Ryde, U.; Veryazov, V.; Widmark, P.-O.; Cossi, M.; Schimmelpfennig, B.; Neogrady, P.; Seijo, L. *Comput. Mater. Sci.* **2003**, *28*, 222–239.
(105) Kepenekian, M.; Robert, V.; Le Guennic, B. *J. Chem. Phys.* **2009**, *131*, 114702.
(106) Beletskaya, I.; Tyurin, V. S.; Yu, A.; Guilard, R.; Stern, C. *Chem. Rev.* **2009**, *109*, 1659–1713.
(107) Fukuzumi, S.; Kojima, T. *J. Mater. Chem.* **2008**, *18*, 1427–1439.
(108) Suslick, K. S.; Bhyrappa, P.; Chou, J. H.; Kosal, M. E.; Nakagaki, S.; Smithenry, D. W.; Wilson, S. R. *Acc. Chem. Res.* **2005**, *38*, 283–291.
(109) Senge, M. O.; Fazekas, M.; Notaras, E. G. A.; Blau, W. J.; Zawadzka, M.; Locos, O. B.; Mhuircheartaigh, E. M. N. *Adv. Mater.* **2007**, *19*, 2737–2774.
(110) Tashiro, K.; Aida, T. *Chem. Soc. Rev.* **2007**, *36*, 189–197.
(111) Choe, Y. K.; Hashimoto, T.; Nakano, H.; Hirao, K. *Chem. Phys. Lett.* **1998**, *295*, 380–388.
(112) Obara, S.; Kashiwagi, H. *J. Chem. Phys.* **1982**, *77*, 3155–3165.
(113) Collman, J. P.; Hoard, J. L.; Kim, N.; Lang, G.; Reed, C. A. *J. Am. Chem. Soc.* **1975**, *97*, 2676–2681.
(114) Goff, H.; La Mar, G. N.; Reed, C. A. *J. Am. Chem. Soc.* **1977**, *99*, 3641–3646.
(115) Kitagawa, T.; Teraoka, J. *Chem. Phys. Lett.* **1979**, *63*, 443–446.
(116) Choe, Y. K.; Nakajima, T.; Hirao, K.; Lindh, R. *J. Chem. Phys.* **1999**, *111*, 3837–3845.
(117) Sontum, S. F.; Case, D. A.; Karplus, M. *J. Chem. Phys.* **1983**, *79*, 2881–2892.
(118) Pierloot, K. *Mol. Phys.* **2003**, *101*, 2083–2094.
(119) Radoń, M.; Pierloot, K. *J. Phys. Chem. A* **2008**, *112*, 11824–11832.
(120) Reiher, M.; Wolf, A. *J. Chem. Phys.* **2004**, *121*, 10945–10956.
(121) For the quintet state, we were informed by Mariusz Radoń that there is a typo in ref 119; thus, the quintet state obtained therein is indeed the $^5A_{1g}$ state with a principle orbital occupancy of $(d_{z^2})^2(d_{xz})^1(d_{yz})^1(d_{xy})^1(d_{x^2-y^2})^1$, as shown in Scheme 2.
(122) Vancoillie, S.; Zhao, H. L.; Radoń, M.; Pierloot, K. *J. Chem. Theory Comput.* **2010**, *6*, 576–582.
(123) Rovira, C.; Kunc, K.; Hutter, J.; Ballone, P.; Parrinello, M. *J. Phys. Chem. A* **1997**, *101*, 8914–8925.
(124) Kozlowski, P. M.; Spiro, T. G.; Bérces, A.; Zgierski, M. Z. *J. Phys. Chem. B* **1998**, *102*, 2603–2608.
(125) Groenhof, A. R.; Swart, M.; Ehlers, A. W.; Lammertsma, K. *J. Phys. Chem. A* **2005**, *109*, 3411–3417.
(126) Liao, M. S.; Watts, J. D.; Huang, M. J. *J. Comput. Chem.* **2006**, *27*, 1577–1592.
(127) Ghosh, A.; Persson, B. J.; Taylor, P. R. *J. Biol. Inorg. Chem.* **2003**, *8*, 507–511.
(128) Ghosh, A.; Taylor, P. R. *Curr. Opin. Chem. Biol.* **2003**, *7*, 113–124.
(129) Ghosh, A.; Taylor, P. R. *J. Chem. Theory Comput.* **2005**, *1*, 597–600.
(130) Jones, D. H.; Hinman, A. S.; Ziegler, T. *Inorg. Chem.* **1993**, *32*, 2092–2095.
(131) Roos, B. O.; Veryazov, V.; Conradie, J.; Taylor, P. R.; Ghosh, A. *J. Phys. Chem. B* **2008**, *112*, 14099–14102.
(132) Chen, H.; Song, J. S.; Lai, W. Z.; Wu, W.; Shaik, S. *J. Chem. Theory Comput.* **2010**, *6*, 940–953.
(133) Oláh, J.; Harvey, J. N. *J. Phys. Chem. A* **2009**, *113*, 7338–7345.
(134) Ghosh, A.; Vangberg, T.; Gonzalez, E.; Taylor, P. R. *J. Porphyrins Phthalocyanines* **2001**, *5*, 345–356.
(135) Schöneboom, J. C.; Neese, F.; Thiel, W. *J. Am. Chem. Soc.* **2005**, *127*, 5840–5853.
(136) Altun, A.; Kumar, D.; Neese, F.; Thiel, W. *J. Phys. Chem. A* **2008**, *112*, 12904–12910.

(137) Radoń, M.; Broclawik, E. *J. Chem. Theory Comput.* **2007**, *3*, 728–734.
(138) Ogliaro, F.; Cohen, S.; de Visser, S. P.; Shaik, S. *J. Am. Chem. Soc.* **2000**, *122*, 12892–12893.
(139) Ogliaro, F.; de Visser, S. P.; Groves, J. T.; Shaik, S. *Angew. Chem., Int. Ed.* **2001**, *40*, 2874–2878.
(140) de Visser, S. P.; Ogliaro, F.; Sharma, P. K.; Shaik, S. *Angew. Chem., Int. Ed.* **2002**, *41*, 1947–1951.
(141) Ogliaro, F.; de Visser, S. P.; Shaik, S. *J. Inorg. Biochem.* **2002**, *91*, 554–567.
(142) Cho, K.-B.; Hirao, H.; Chen, H.; Carvajal, M. A.; Cohen, S.; Derat, E.; Thiel, W.; Shaik, S. *J. Phys. Chem. A* **2008**, *112*, 13128–13138.
(143) (a) Newcomb, M.; Zhang, R.; Chandrasena, R. E.; Halgrimson, J. A.; Horner, J. H.; Makris, T. M.; Sligar, S. G. *J. Am. Chem. Soc.* **2006**, *128*, 4580–4581. (b) Sheng, X.; Horner, J. H.; Newcomb, M. *J. Am. Chem. Soc.* **2008**, *130*, 13310–13320. (c) Sheng, X.; Zhang, H. M.; Im, S.-C.; Horner, J. H.; Waskell, L.; Hollenberg, P. F.; Newcomb, M. *J. Am. Chem. Soc.* **2009**, *131*, 2971–2976. (d) Wang, Q.; Sheng, X.; Horner, J. H.; Newcomb, M. *J. Am. Chem. Soc.* **2009**, *131*, 10629–10636.
(144) (a) Watanabe, Y. *J. Biol. Inorg. Chem.* **2001**, *6*, 846–856. (b) Pan, Z. Z.; Zhang, R.; Fung, L. W.-M.; Newcomb, M. *Inorg. Chem.* **2007**, *46*, 1517–1519. (c) Pan, Z. Z.; Wang, Q.; Sheng, X.; Horner, J. H.; Newcomb, M. *J. Am. Chem. Soc.* **2009**, *131*, 2621–2628.
(145) Balabanov, N. B.; Peterson, K. A. *J. Chem. Phys.* **2005**, *123*, 064107.
(146) Neese, F. *Coord. Chem. Rev.* **2009**, *253*, 526–563.
(147) Jain, R.; Chan, M. K. *J. Biol. Inorg. Chem.* **2003**, *8*, 1–11.
(148) Pauling, L.; Coryell, C. D. *Proc. Natl. Acad. Sci. U.S.A.* **1936**, *22*, 210–216.
(149) Chen, H.; Iketa-Saito, M.; Shaik, S. *J. Am. Chem. Soc.* **2008**, *130*, 14778–14790.
(150) Weiss, J. J. *Nature* **1964**, *202*, 83–84.
(151) McClure, D. S. *Radiat. Res. Suppl.* **1960**, *2*, 218–342.
(152) Yamamoto, S.; Kashiwagi, H. *Chem. Phys. Lett.* **1989**, *161*, 85–89.
(153) Yamamoto, S.; Kashiwagi, H. *Chem. Phys. Lett.* **1993**, *205*, 306–312.
(154) Harcourt, R. D. *Chem. Phys. Lett.* **1990**, *167*, 374–377.
(155) Jensen, K. P.; Roos, B. O.; Ryde, U. *J. Inorg. Biochem.* **2005**, *99*, 45–54, 978 (erratum).
(156) Ribas-Ariño, J.; Novoa, J. J. *Chem. Commun.* **2007**, 3160–3162.
(157) Franzen, S. *Proc. Natl. Acad. Sci. U.S.A.* **2002**, *99*, 16754–16759.
(158) Jensen, K. P.; Ryde, U. *J. Biol. Chem.* **2004**, *279*, 14561–14569.
(159) Nakashima, H.; Hasegawa, J. Y.; Nakatsuji, H. *J. Comput. Chem.* **2006**, *27*, 426–433.
(160) Siegbahn, P. E. M.; Blomberg, M. R. A.; Chen, S.-L. *J. Chem. Theory Comput.* **2010**, *6*, 2040–2044.
(161) Spiro, T. G.; Wasbotten, I. H. *J. Inorg. Biochem.* **2005**, *99*, 34–44.
(162) Ortiz de Montellano, P. R. *Acc. Chem. Res.* **1998**, *31*, 543–549.
(163) Colas, C.; Ortiz de Montellano, P. R. *Chem. Rev.* **2003**, *103*, 2305–2332.
(164) Unno, M.; Matsui, T.; Ikeda-Saito, M. *Nat. Prod. Rep.* **2007**, *24*, 553–570.
(165) Matsui, T.; Unno, M.; Ikeda-Saito, M. *Acc. Chem. Res.* **2010**, *43*, 240–247.
(166) Matsui, T.; Iwasaki, M.; Sugiyama, R.; Unno, M.; Ikeda-Saito, M. *Inorg. Chem.* **2010**, *49*, 3602–3609.
(167) (a) Nathan, C. *FASEB J.* **1992**, *6*, 3051–3064. (b) Griffith, O. W.; Stuehr, D. J. *Annu. Rev. Physiol.* **1995**, *57*, 707–736. (c) Marletta, M. A.; Hurshman, A. R.; Rusche, K. M. *Curr. Opin. Chem. Biol.* **1998**, *2*, 656–663. (d) Groves, J. T.; Wang, C. C. Y. *Curr. Opin. Chem. Biol.* **2000**, *4*, 687–695. (e) Alderton, W. K.; Cooper, C. E.; Knowles, R. G. *Biochem. J.* **2001**, *357*, 593–615. (f) Rosen, G. M.; Tsai, P.; Pou, S. *Chem. Rev.* **2002**, *102*, 1191–1199. (g) Li, Y. Y.; Poulos, T. L. *J. Inorg. Biochem.* **2005**, *99*, 293–305. (h) Crane, B. R.; Sudhamsu, J.; Patel, B. A. *Annu. Rev. Biochem.* **2010**, *79*, 445–470.
(168) Garthwaite, J.; Boulton, C. L. *Annu. Rev. Physiol.* **1995**, *57*, 683–706.
(169) Westcott, B. L.; Enemark, J. L. In *Inorganic Electronic Structure and Spectroscopy*; Solomon, E. I., Lever, A. B. P., Eds.; Wiley: New York, 1999; Vol. 2, pp 403−450.
(170) Radoń, M.; Broclawik, E.; Pierloot, K. *J. Phys. Chem. B* **2010**, *114*, 1518–1528.
(171) Conradie, J.; Ghosh, A. *J. Phys. Chem. B* **2007**, *111*, 12621–12624.
(172) As seen from many applications of MR/MC methods in refs 118, 119, 122, 131, 132, 136, 149, 155, 156, and 170, the double-shell effect was accounted for by including some 4d iron orbitals in the active space. There are at least two reasons that, for large systems like heme-related complexes, including the total shell of iron 4d orbitals could be problematic and/or impractical. The first reason is that for large systems it is very easy to reach the limit of current CASPT2 calculation in terms of the active-space size, which is currently about 16 active orbitals. As such, including the full set of 4d orbitals could be computationally impossible. The second reason is the active space instability issue observed in some of the studies in refs 119 and 170 and observed also by the present authors. Thus, inclusion of iron 4d orbitals corresponding to empty 3d orbitals causes instability of the active space, which manifests either as convergence failure of the CASSCF calculation or changes of the intended active space. Fortunately, as found quite early in ref 89, 4d orbitals corresponding to empty 3d orbitals have a very small effect on the CASPT2 calculation and only those corresponding to doubly occupied 3d orbitals could contribute significantly in CASPT2 calculations. Thus, it should be safe to include only 4d orbitals corresponding to doubly occupied 3d orbitals. It should also be pointed out that, according to our own experience, the most important 4d orbitals are those whose corresponding 3d occupancies change between 1 and 2 in the calculated states. One typical example mentioned frequently in this review is two states with occupancies $(d_{x^2-y^2})^1(d_{xy})^1$ and $(d_{x^2-y^2})^0(d_{xy})^2$, where $4d_{xy}$ is important in active space for the calculated energy gap between these two states. From previous calibration (see ref 89), it is known that the double-shell effect decreases usually with increasing oxidation state of the transition metal (less population on the metal).
(173) Malmqvist, P. Å.; Pierloot, K.; Shahi, A. R. M.; Cramer, C. J.; Gagliardi, L. *J. Chem. Phys.* **2008**, *128*, 204109.
(174) Rittle, J.; Green, M. T. *Science* **2010**, *330*, 933–937.
(175) (a) Edmiston, C.; Ruedenberg, K. *Rev. Mod. Phys.* **1963**, *35*, 457–465. (c) See applications in MCSCF: Schmidt, M. W.; Gordon, M. S. *Annu. Rev. Phys. Chem.* **1998**, *49*, 233–266.
(176) Shaik, S. S. *J. Am. Chem. Soc.* **1981**, *103*, 3692–3701.
(177) Shaik, S.; Hiberty, P. C. In *A Chemist's Guide to Valence Bond Theory*; John Wiley & Sons Inc.: Hoboken NJ, 2008; Chapter 4, pp 81−93.
(178) Hiberty, P. C.; Leforestier, C. *J. Am. Chem. Soc.* **1978**, *100*, 2012–2017.
(179) Karafiloglu, P.; Ohanessian, G. *J. Chem. Educ.* **1991**, *68*, 583–586.
(180) Bachler, V.; Schaffner, K. *Chem.—Eur. J.* **2000**, *6*, 959–970.
(181) Moffitt, W. *Proc. R. Soc. London, Ser. A* **1953**, *218*, 486–506.
(182) Neese, F.; Petrenko, T.; Ganyushin, D.; Olbrich, G. *Coord. Chem. Rev.* **2007**, *251*, 288–327.
(183) Chen, H.; Lai, W. Z.; Shaik, S. *J. Phys. Chem. Lett.* **2010**, *1*, 1533–1540.
(184) Geng, C.; Ye, S.; Neese, F. *Angew. Chem. Int. Ed.* **2010**, *49*, 5717–5720.
(185) Shaik, S.; Chen, H.; Janardanan, D. *Nature Chem.* **2011**, *3*, 19–27.